IOP Publishing J. Phys. Complex. 5 (2024) 015022 https://doi.org/10.1088/2632-072X/ad353b

Journal of Physics: Complexity

OPEN ACCESS

RECEIVED
10 February 2024

REVISED
13 March 2024

ACCEPTED FOR PUBLICATION
18 March 2024

PUBLISHED
28 March 2024

PAPER

Higher-order connection Laplacians for directed simplicial complexes

Xue Gong[1,2,3,4], **Desmond J Higham**[1,2], **Konstantinos Zygalakis**[1,2] **and Ginestra Bianconi**[3,5,*]

[1] School of Mathematics, University of Edinburgh, Edinburgh EH9 3FD, United Kingdom
[2] The Maxwell Institute for Mathematical Sciences, Edinburgh EH8 9BT, United Kingdom
[3] The Alan Turing Institute, 96 Euston Rd, London NW1 2DB, United Kingdom
[4] Division of Mathematics, Nanyang Technological University, 50 Nanyang Avenue, Singapore 639798, Singapore
[5] School of Mathematical Sciences, Queen Mary University of London, London E1 4NS, United Kingdom
[*] Author to whom any correspondence should be addressed.

E-mail: g.bianconi@qmul.ac.uk

Keywords: connection Laplacian, simplicial complex, higher-order diffusion, Hodge Laplacian, magnetic Laplacian

Abstract

Higher-order networks encode the many-body interactions existing in complex systems, such as the brain, protein complexes, and social interactions. Simplicial complexes are higher-order networks that allow a comprehensive investigation of the interplay between topology and dynamics. However, simplicial complexes have the limitation that they only capture undirected higher-order interactions while in real-world scenarios, often there is a need to introduce the direction of simplices, extending the popular notion of direction of edges. On graphs and networks the Magnetic Laplacian, a special case of connection Laplacian, is becoming a popular operator to address edge directionality. Here we tackle the challenge of handling directionality in simplicial complexes by formulating higher-order connection Laplacians taking into account the configurations induced by the simplices' directions. Specifically, we define all the connection Laplacians of directed simplicial complexes of dimension two and we discuss the induced higher-order diffusion dynamics by considering instructive synthetic examples of simplicial complexes. The proposed higher-order diffusion processes can be adopted in real scenarios when we want to consider higher-order diffusion displaying non-trivial frustration effects due to conflicting directionalities of the incident simplices.

1. Introduction

Higher-order networks [1–4] are attracting increasing attention as they have the ability to encode for the interactions [5] among two or more nodes of complex systems and to display a rich interplay between topology and dynamics [6, 7]. Higher-order networks include hypergraphs [8–12] as well as simplicial complexes. Simplicial complexes are higher-order networks that are amenable to a comprehensive higher-order topological treatment revealing the topology of data [13–18] leading to applications in neuroscience [19–21], biology [22–25], sensor networks [26, 27], and computer graphics [28, 29]. Moreover, the algebraic topology of simplicial complexes is drastically changing our understanding of the dynamical state of simple and higher-order networks. Until recently the dynamical description of the network has taken almost exclusively a node (vertex)-centric approach where only the nodes are associated with dynamical variables. The investigation of the dynamical state of simplicial complexes has instead revealed that this is only a special case and that in general each simplex (higher-order interaction) can be associated with a dynamical variable leading to the notion of topological signals. This change of paradigm has lead to novel understanding of topological synchronization [30–34] and higher-order diffusion dynamics [35–38] and to novel signal processing [39–41] and topological neural network algorithms [42, 43]. In particular, higher-order diffusion dynamics is among the most basic topological dynamical processes, describing diffusion from n-dimensional simplices to n-dimensional simplices going either one dimension up or one

dimension down. For instance, for $n = 1$ higher-order diffusion captures diffusion from edges to edges going either through nodes or through triangles. The main operator driving higher-order diffusion is the Hodge Laplacian [44–46] which encodes important information about the simplicial complex topology and is a key player in understanding the interplay between topology and dynamics.

Simplicial complexes have an important limitation as they usually encode only for undirected higher-order interactions. However, in applications, there is an increasing need to include also directional simplicial complexes [21, 31, 47]. Additionally, from the perspective of algebraic topology, an important challenge is related to the definition of the topology of directed simplicial complexes for which several proposals have been recently suggested [48–50].

While the investigation of directionality on simplicial complexes is only in its infancy, on networks considering directional edges is a much more widely explored topic. Among many different approaches, recently it has been shown that the Magnetic Laplacian is a fundamental algebraic operator that captures the directionalities of the edges while preserving a real and positive spectrum. The Magnetic Laplacian has its roots in theoretical physics and gauge theory [51–54], but recently has been shown to provide a valuable tool for node embeddings [55–59] and for the formulation of new neural network architectures [60]. The Magnetic Laplacian is a Hermitian operator that acts on complex-valued variables associated with the nodes and enforces a rotation of the complex phase at every edge. Thus the Magnetic Laplacian can be interpreted as a Laplacian with complex-valued weights on its edges, which is one of the emerging topics in network theory [59, 61, 62]. Interestingly, the Magnetic Laplacian can be seen as a generalization of the Connection Laplacian [63–65] acting on a vector field defined on each node of the network and inducing a rotation of the vector in correspondence of each edge.

In this work, we are motivated by the success of the Magnetic Laplacian in handling directed networks and we formulate Higher-order Connection Laplacians for the study of directed simplicial complexes of dimension two. The 1-order Connection Laplacians, for example, rotate complex valued 2-dimensional vectors associated with edges when transported across a node or a triangle according to rules depending on the relative directions of the simplicial complex. In particular, we show that in order to take into account all possible configurations of relative directions of simplices we need to make use of the Pauli matrices as well as of an additional rotation of the complex phases. The higher-order Connection Laplacians are here adopted in order to define higher-order diffusion on directed simplicial complexes that can reveal important dynamical effects induced by the 'frustration' of the relative directions of the simplices as demonstrated from the study of instructive synthetic examples.

By formulating the higher-order Connection Laplacians this work demonstrates that a much unexplored yet very promising research direction in higher-order networks is the investigation of the dynamics of topological signals combined with rich algebraic structures. Other examples of this emerging topic are the adoption of the Dirac operator [66] and its associated gamma matrices [67] to study for instance Turing and Dirac-induced patterns of topological signals, higher-order synchronization dynamics [68, 69], the use of sheaves in opinion dynamics [70], and the extensive literature on physics-inspired neural networks [43, 71]. The mathematical methods that we present may also be used to develop random-walk centrality measures [72] and embeddings [55] for directed higher-order networks.

2. Combinatorial, connection and magnetic Laplacians on graphs

We consider a graph $G = (V, E)$ with N_0 vertices and N_1 edges. We are interested in the scenario in which this graph describes a real-world complex system; in this case, it is also referred to as a network. Here we discuss three definitions of Laplacians: the Combinatorial Graph Laplacian [73–76], the Connection Laplacian [63, 64], and the Magnetic Laplacian [55, 57]. The Laplacians are algebraic topology operators that can be used to describe diffusion on the graph and have wide applications in network science [57, 77, 78], non-linear dynamics [35, 36, 79], as well as in signal processing [33, 80–82] and machine learning [73, 83, 84].

2.1. Combinatorial graph Laplacian

The Combinatorial graph Laplacian $L^{(0)}$ [73, 76] is probably the most widely used Laplacian for undirected graphs and networks. Let us assume $G = (V, E)$ is simple (unweighted, undirected and without self-loops and reciprocated edges) and has adjacency matrix $A^{(0)}$; then the Combinatorial Graph Laplacian $L^{(0)}$ is the $N_0 \times N_0$ matrix defined as

$$L^{(0)} = D^{(0)} - A^{(0)}, \tag{1}$$

where $D^{(0)}$ is the diagonal matrix having the degrees of the vertices in the network, i.e. $D^{(0)}_{ii} = \sum_{j \in V}^{N_0} A^{(0)}_{ij}$ for all vertices i of the graph. This Laplacian provides the paradigmatic example of Laplacian operator that

reflects the graph's discrete geometry and topology in its spectral properties [76] strongly affecting the dynamics unfolding on the graph. Therefore $L^{(0)}$ provides a key way to relate the structure and dynamics of networks and has a key role in Network Science [79] and Machine Learning [85]. However, a limitation of the Combinatorial Graph Laplacian is the fact that the original definition only applies to undirected networks. In the following, we will discuss in detail the Magnetic Laplacian, which addresses this limitation by the adoption of Hermitian matrices.

2.2. Magnetic Laplacian on directed graph

Consider an unweighted directed graph $G = (V, E)$ with vertex set V and directed edge set E connecting pairs of distinct vertices (no self-loop and no reciprocated edges). Let a indicate the binary directed adjacency matrix, and let us define A as the adjacency matrix of its corresponding unweighted network, i.e. $A^{(0)}_{ij} = 1$ if (i, j) exists (in any direction) and $A^{(0)}_{ij} = 0$ otherwise. The Magnetic Laplacian [51, 55] $L^{(g)}$ is a $N_0 \times N_0$ Hermitian matrix defined as

$$L^{(g)} = D^{(0)} - T^{(g)} \circ A^{(0)} \tag{2}$$

where $\circ$ indicates the Hadamard product and $T^{(g)}_{ij} = \exp(\mathrm{i}\delta_{ij})$ assigns a rotation in the complex phase to a directed link, $\delta_{ij} = -2\pi g(a_{ij} - a_{ji})$, with g being a constant parameter. Therefore, $\delta_{ij} = -2\pi g$ if $i \to j$; $\delta_{ij} = 2\pi g$ if $i \leftarrow j$; and $\delta_{ij} = 0$ otherwise. Thus a non-zero value of δ_{ij} arises from directed (i.e. unreciprocated) edges and determines the phase change that occurs when crossing a link from node i to node j. Additionally, the definition of the Magnetic Laplacian involves the diagonal degree matrix $D^{(0)}$ is defined as in the previous paragraph.

For convenience, denote $\delta = 2\pi g$. Then

$$T^{(g)}_{ij} = \begin{cases} e^{-\mathrm{i}\delta}, & \text{if } i \to j \\ e^{\mathrm{i}\delta}, & \text{if } j \to i \\ 1, & \text{otherwise.} \end{cases} \tag{3}$$

The Magnetic Laplacian acts on complex-valued cochains that can be represented as the vector $\boldsymbol{\nu} \in \mathbb{C}^{N_0}$, having complex values on each of the nodes. The Magnetic Laplacian is associated with the quadratic form

$$\boldsymbol{\nu}^{\dagger} L^{(g)} \boldsymbol{\nu} = \frac{1}{2} \sum_{i,j} A_{ij} \| \nu_i - T^{(g)}_{ij} \nu_j \|^2. \tag{4}$$

It is therefore apparent that the Magnetic Laplacian has a real and non-negative spectrum. Its associated quadratic form can be combined with machine learning algorithms to define efficiently network embeddings [55–59] that can reveal for instance non-trivial cyclic patterns or connections among clusters or communities of the network and neural networks [60].

2.3. Connection Laplacian

The Connection Laplacian [63–65] generalizes the definition of the Magnetic Laplacian and can be used to describe the motion of d-dimensional vectors along edges. The Connection Laplacian, denoted $L^{(c)}_0$, is a $N_0 \times N_0$ matrix defined as

$$L^{(c)}_0 = D^{(0)} \otimes I_d - T^{[0],c} \circ \left(A^{(0)} \otimes \mathbf{1}_d \right), \tag{5}$$

where $\mathbf{1}_d$ is the $d \times d$ matrix having all elements equal to one, and the rotation matrix $T^{[0],C}$ is given by $T^{[0],c}_{ij} = O_{ij}$ where $O_{ij} \in \mathbb{R}^{d \times d}$ is the rotation matrix which represents the orthogonal transformation $SO(d)$ satisfying $O_{ij} O_{ji} = I_d$.

The Connection Laplacian acts on real-valued cochains $\boldsymbol{\nu}$ where each element of the cochain associated to a vertex i is a vector $\nu_i \in \mathbb{R}^d$. Thus the quadratic form associated with the Connection Laplacian is given by

$$\boldsymbol{\nu}^{T} L^{(c)} \boldsymbol{\nu} = \frac{1}{2} \sum_{i,j \in V} A_{ij} \| \nu_i - O_{ij} \nu_j \|^2. \tag{6}$$

A Connection Laplacian is called *consistent* if, for every cycle in the graph, the total rotation is equivalent to the identity matrix. This property ensures that one can always rotate back to the same phase after completing

any directed cycle [86]. Moreover, when a Connection Laplacian is consistent, there exist exactly d eigenvalues with a value of 0.

It can be easily shown that the Magnetic Laplacian [55, 57] is a special case of Connection Laplacian for directed graphs with a $U(1)$ or $SO(2)$ transformation. As we will see in the following, our manuscript proposes to generalize the notion of Graph Connection Laplacian to directed simplicial complexes with the goal of capturing in the spectral properties of these operators the information encoded in the directions of their simplices, in the same spirit as the use of the Magnetic Laplacian to capture the directionalities of edges in graphs and networks.

3. Simplicial complexes

Simplicial complexes are a class of higher-order networks that encode higher-order interactions in complex systems. In this work, we will consider 2-dimensional simplicial complexes formed by vertices (0-simplices), edges (1-simplices) and triangles (2-simplices). More formally, a *simplex* of dimension k (or k-simplex) is formed by $n+1$ vertices, and the *face* of a simplex is a simplex of dimension $k' < k$ formed by a proper subset of the vertices of the original simplex. A simplicial complex $\mathcal{K}$ is a set of simplices closed under the inclusion of the faces of each of its simplices. The *dimension* of a simplicial complex is the largest dimension of its simplices. The use of simplicial complexes [1–4] is becoming popular in Network Science and complex systems research as it allows us to model complex systems such as the brain, protein assemblies, or social interactions, where each simplex characterizes a given higher-order interaction among their elements.

Simplicial complexes allow for higher-order extensions of Combinatorial Graph Laplacians called Hodge Laplacians that can reveal important properties of higher-order diffusion between n-simplices to n-simplices. In order to define the Hodge Laplacian it is important to associate to each simplex an orientation, typically chosen to be induced by the node labels. Here and in the following, unless clearly specified, we always adopt this convention as it has the advantage that the spectral properties of the Hodge Laplacians will be independent of the vertex labelling. Note most importantly that the notion of orientation is distinct from the notion of direction. For instance an oriented 1-dimensional simplex (an oriented graph) will attribute to each edge an orientation and not a direction. The orientation can be used for instance to determine if a flux through an edge is positive or negative; for instance if the edge $[1,2]$ is oriented positively, a flux going from vertex 1 to vertex 2 will be positive, and a flux from vertex 2 to vertex 1 will be negative. From this example, it is clear that the orientation of an edge is a different notion with respect to direction, as a directed link will allow only flux to go in one direction.

Hodge Laplacians are receiving increased interest because of their ability to encode the topology of simplicial complexes at the same time as offering the correct algebraic topology operator to define higher-order diffusion and to model, treat and process higher-order topological signals. In particular, the k-order Hodge Laplacian acts on k cochains, which can be represented as vectors assigning a dynamical value to each k-simplex of the simplicial complex. The action of the k-Laplacian on the k-cochain can describe diffusion from k-simplex to k-simplex passing either though $(k-1)$ or to $(k+1)$ simplices.

Here our intention is to give a brief computational introduction to Hodge Laplacians without giving the full background of these important algebraic topology operators. For further information we recommend the following literature, devoted to their spectral properties: [44, 46, 87].

In order to provide an operational definition of Hodge Laplacians let us introduce some notation. We consider the finite oriented simplicial complex $\mathcal{K}$ formed by N_k simplices of dimension k, each denoted as α_k^i with $1 \leqslant i \leqslant N_k$. Two distinct k-simplices α_k^i and α_k^j are *upper adjacent* if they both are faces of a $(k+1)$-simplex, also known as a co-face. Two simplices that are upper-adjacent and have the same relative orientation with respect to the common co-face are indicated as $\sigma_k^1 \sim_U \sigma_k^2$, while otherwise we indicate $\alpha_k^i \not\sim_U \alpha_k^j$. Two distinct k-simplices are *lower adjacent* if they share a common face. Two simplices that are lower-adjacent and have the same relative orientation with respect to the common face are indicated as $\sigma_k^1 \sim_L \sigma_k^2$, while otherwise, we indicate $\alpha_k^i \not\sim_L \alpha_k^j$. The k-order Hodge Laplacian is a $N_k \times N_k$ matrix given by

$$\mathcal{L}_k = \mathcal{L}_k^{up} + \mathcal{L}_k^{down}, \tag{7}$$

where we use the convention $\mathcal{L}_0^{c,down} = 0$ and in all other cases the up and the down Hodge Laplacians $\mathcal{L}_k^{up}$ and $\mathcal{L}_k^{c,down}$ have elements

$$\left[\mathcal{L}_k^{up}\right]_{ij} = \begin{cases} \deg_U\left(\alpha_k^i\right), & \text{if } i=j \\ 1, & \text{if } \alpha_k^i \sim_U \alpha_k^j \\ -1, & \text{if } \alpha_k^i \not\sim_U \alpha_k^j \\ 0, & \text{otherwise;} \end{cases}, \quad \left[\mathcal{L}_k^{down}\right]_{ij} = \begin{cases} k+1, & \text{if } i=j \\ 1, & \text{if } \alpha_k^i \sim_L \alpha_k^j \\ -1, & \text{if } \alpha_k^i \not\sim_L \alpha_k^j \\ 0, & \text{otherwise.} \end{cases} \tag{8}$$

From this definition, it follows that as long as $k=0$ the Hodge Laplacian reduces to the Combinatorial Graph Laplacian while for $k>0$ the Hodge Laplacian has elements

$$[\mathcal{L}_k]_{ij}=\begin{cases}\deg_U\left(\alpha_k^i\right)+k+1, & \text{if } i=j\\ 1, & \text{if } \alpha_k^i\sim_L\alpha_k^j \text{ and they are not upper adjacent}\\ -1, & \text{if } \alpha_k^i\not\sim_L\alpha_k^j \text{ and they are not upper adjacent}\\ 0, & \text{otherwise.}\end{cases} \tag{9}$$

Hodge Laplacians encode fundamental topological properties of the simplicial complex. In particular, one of the most celebrated properties of Hodge Laplacians is that the dimension of the kernel of the n-Hodge Laplacian is given by the nth Betti number. Another crucial property of Hodge Laplacians is that they obey Hodge decomposition and thus allow, for instance, the decomposition of edge signals into harmonic, solenoidal, and irrotational components.

4. Higher-order connection Laplacians of 2-dimensional simplicial complexes

Hodge Laplacians constitute a powerful tool to study the topology of higher-order networks, however, they have the important limitation of only applying to undirected (although oriented) simplicial complexes. This is a drawback for studying real higher-order networks and represents also a significant challenge in mathematics in general and applied topology in particular.

Here our goal is to propose the study of Higher-order Connection Laplacians of 2-dimensional simplicial complexes, in order to capture spectral properties that are induced by introducing the directionality of the simplices. In doing so we are inspired by the recognized role of the Magnetic Laplacian as the key algebraic topology operator to handle directionality in the graph setting while preserving a real and non-negative spectrum. In particular, we will define the k-order Connection Laplacian that will determine how vectors defined on simplices are transformed when hopping though upper or lower adjacent simplices (see figure 1). As we will see the 0-Connection Laplacian can be defined trivially as the Combinatorial Graph Laplacian of the underlying network skeleton of the simplicial complex, i.e. the graph formed only by vertices and edges of the simplicial complex. Therefore, this operator can be defined on complex-valued 0-cochains assigned to each vertex of the graph. In order to take into account all possible configurations induced by the directions of edges and triangles, the 1-Connection Laplacian will however, require us to lift the dimensionality of the 1-cochain to a 2-dimensional complex valued vector defined on each edge of the simplicial complex. The 2-Connection Laplacian will be acting on a 2-cochain taking as well a 2-dimensional complex valued vector on each triangle of the simplicial complex. However, another difficulty arises, as to define an *Hermitian* 2-Connection Laplacian we will have to limit our discussion to simplicial complexes that tessellate 2-dimensional orientable manifolds.

4.1. Higher-order connection Laplacian for 2-dimensional simplicial complexes

Consider a simplicial complex $\mathcal{K}$ of dimension 2, including three different types of simplices: nodes, edges, and triangles. We assume that the simplicial complex is unweighted and directed. The undirected version of this simplicial complex is given by the same simplicial complex that is oriented instead of directed, with nodes, edges, and triangles having an orientation induced by the vertex labels, and with nodes having a trivial positive orientation. The directed simplicial complex has both edges and triangles associated with a direction, either concordant or discordant with their own orientation of its undirected version. Here our goal is to generalize the notion of the Connection Laplacian to higher-order networks in order to capture the information encoded in the directionality of the simplices and to define a higher-order diffusion that takes into account the directions of the simplices on top of their orientation. Note however that we do not intend here to define the topology of the directed simplicial complexes, and that the Higher-order Connection Laplacians have significant differences with respect to the Hodge Laplacian of undirected networks. One of the main differences is that in general the Higher-order Connection Laplacian will not obey Hodge decomposition, and in addition, the 1-up Connection Laplacian and the 1-down Connection Laplacian might not even commute.

4.2. 0-up connection Laplacian

For the 0-Connection Laplacian, by adopting a minimal assumption, we propose to use the Magnetic Laplacian of the directed simplicial complex skeleton formed exclusively by the vertices and the directed edges of the simplicial complex. The graph Magnetic Laplacian uses complex numbers to encode the direction of the edges and simultaneously builds a Hermitian operator with real eigenvalues that can be useful for machine learning applications. Note that the vertices of a network have all the same (trivial)

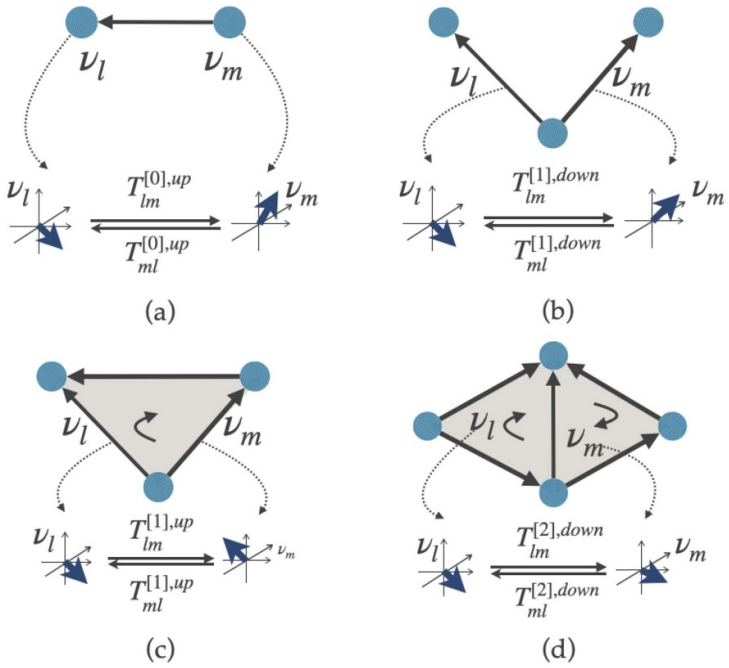

Figure 1. Higher-order Connection Laplacians rotate vectors along nodes, edges, or triangles. (a) 0-up Connection Laplacian rotates vectors defined on vertices along edges. (b) 1-down Connection Laplacian rotates vectors defined on edges along nodes. (c) 1-up Connection Laplacian rotates vectors defined on edges along triangles. (d) 2-down Connection Laplacian rotates vectors defined on triangles along edges.

direction so that in a network it is sufficient to take into account the two different directions of the edges (accounted for by the sign of the argument of the corresponding complex number). It follows that the matrix element $L_{ij}^{(g)}$ depends only on the direction of the link (i,j) which can be $i \to j$ or $i \leftarrow j$. A question that arises is how to leverage this to define the 1-order Connection Laplacian or even the 2-down Connection Laplacian.

4.3. 1-up connection Laplacian

When one considers the 1-Connection Laplacian, the situation is much richer than at the network level. Indeed the matrix element $L_{[ij][jk]}^{[1],up}$ describing higher-order diffusion between edge $[i,j]$ and edge $[j,k]$ will not only depend on the direction of the triangle $[i \to j \to k]$ and $[k \to j \to i]$ but also on the directions of the edges $[i,j]$ and $[j,k]$. Taking into account all the possible combinations of the directions of the two edges and the upper incident triangle leads to eight possible configurations (see figure 1). If follows that it is not possible to use only the phase of complex numbers to distinguish between these 8 possible configurations. We therefore consider a complex-valued $1-$*cochain* $\boldsymbol{\nu}$ of elements $\nu_\ell \in \mathbb{C}^2$ defined on each edge $\ell = [i,j]$ of the simplicial complex. We then consider a 1-Connection Laplacian that will enforce rotations induced by the four Pauli matrices in conjunction with rotation of the complex phases of the elements ν_ℓ. Since the Pauli matrices, together with the identity matrix, form a set of four, and the complex phase can rotate in two different directions, we can take into account all eight combinatorial options induced by the direction of the two incident edges and the shared triangle. This greatly enriches the complexity of the definition of the 1 Connection Laplacian. To construct the 1-up Connection Laplacian, we start by constructing the Bochner matrix $\boldsymbol{\mathcal{B}}_1^{up}$ [88] of the 1-up Hodge Laplacian $\mathcal{L}_{[1]}^{c,up}$ of the undirected version of the simplicial complex whose elements are given by

$$\left[\mathcal{B}_1^{up}\right]_{lm} = \begin{cases} \left[\mathcal{L}_1^{c,up}\right]_{lm} & \text{if } l \neq m, \\ \sum_n \left|\left[\mathcal{L}_1^{c,up}\right]_{ln}\right| & \text{if } l \neq m. \end{cases} \tag{10}$$

This Bochner matrix is semi-definite positive and can be written as the difference of a diagonal part $D^{(1),up}$ and a non-diagonal part A_1^{up}, i.e.

$$\mathcal{B}_{[1]}^{up} = D^{(1),up} - A_{[1]}^{up}. \tag{11}$$

Here, the diagonal matrix $D^{(1),up}$ has elements given by $[D^{(1),up}]_{ll} = 2\deg_U(\sigma_1^l)$, which are twice the number of triangles incident to edge l.

Table 1. Schematic representation of the eight configurations induced by the directionality of edges and triangles which are distinguished by the Higher-order Connection Laplacian $\mathcal{L}_1^{c,up}$.

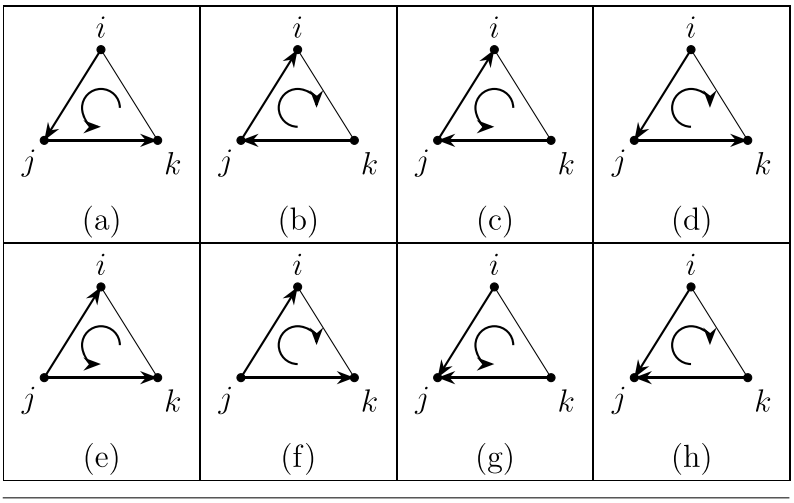

Moreover by indicating with α_1^l, α_1^m the lth and the mth oriented edges (1-simplices), we have

$$\left[A_1^{up}\right]_{lm} = \begin{cases} 0, & \text{if } l = m \\ -1, & \text{if } \alpha_1^l \sim_U \alpha_1^m \\ 1, & \text{if } \alpha_1^l \not\sim_U \alpha_1^m \\ 0, & \text{otherwise.} \end{cases} \tag{12}$$

With these definitions we define the 1-up Connection Laplacian, $\mathcal{L}_1^{c,up}$, acting on 1-cochains $\boldsymbol{\nu}$ of elements $\nu_l \in \mathbb{C}^2$ associated to the generic edge α_1^l of the directed simplicial complex as:

$$\mathcal{L}_1^{c,up} = D^{(1),up} \otimes I_2 - T^{[1],up} \circ \left(A_1^{up} \otimes \mathbf{1}_2\right), \tag{13}$$

where $\mathbf{1}_2$ is the 2×2 matrix having all elements equal to one. The rotation matrix $T^{[1],up}$ is a $2N_1 \times 2N_1$ matrix that enforces a different type of rotation depending on the directions of the two incident edges and the direction of the incident triangle. Specifically, for a given choice of $\delta \in [0, 2\pi)$ we define $T^{[1],up}_{(ij),(jk)}$ as:

$$T^{[1],up}_{(ij),(jk)} = \begin{cases} e^{-\mathbf{i}\delta}\boldsymbol{\sigma}_0, & \text{if } i \to j, j \to k, i \to j \to k \quad \text{(a)} \\ e^{\mathbf{i}\delta}\boldsymbol{\sigma}_0, & \text{if } j \to i, k \to j, i \leftarrow j \leftarrow k \quad \text{(b)} \\ e^{-\mathbf{i}\delta}\boldsymbol{\sigma}_x, & \text{if } j \to i, k \to j, i \to j \to k \quad \text{(c)} \\ e^{\mathbf{i}\delta}\boldsymbol{\sigma}_x, & \text{if } i \to j, j \to k, i \leftarrow j \leftarrow k \quad \text{(d)} \\ e^{-\mathbf{i}\delta}\boldsymbol{\sigma}_y, & \text{if } j \to i, j \to k, i \to j \to k \quad \text{(e)} \\ e^{\mathbf{i}\delta}\boldsymbol{\sigma}_y, & \text{if } j \to i, j \to k, i \leftarrow j \leftarrow k \quad \text{(f)} \\ e^{-\mathbf{i}\delta}\boldsymbol{\sigma}_z, & \text{if } i \to j, k \to j, i \to j \to k \quad \text{(g)} \\ e^{\mathbf{i}\delta}\boldsymbol{\sigma}_z, & \text{if } i \to j, k \to j, i \leftarrow j \leftarrow k \quad \text{(h)} \\ \boldsymbol{\sigma}_0, & \text{otherwise,} \end{cases} \tag{14}$$

where the letters refer to the labeling of the configurations in table 1. Here, $\boldsymbol{\sigma}$ are the Pauli matrices

$$\boldsymbol{\sigma}_0 = \begin{pmatrix} 1 & 0 \\ 0 & 1 \end{pmatrix}, \quad \boldsymbol{\sigma}_x = \begin{pmatrix} 0 & 1 \\ 1 & 0 \end{pmatrix}, \quad \boldsymbol{\sigma}_y = \begin{pmatrix} 0 & -i \\ i & 0 \end{pmatrix} \quad \boldsymbol{\sigma}_z = \begin{pmatrix} 1 & 0 \\ 0 & -1 \end{pmatrix}. \tag{15}$$

Motivated by the Magnetic Laplacian setting, we view δ as a phase rotation, and we aim to study the simplicial complex for various choices of δ.

From this definition of the 1-up Connection Laplacian it is straightforward to express the associated quadratic form as

$$\boldsymbol{\nu}^\dagger \mathcal{L}_1^{c,up} \boldsymbol{\nu} = \frac{1}{2}\left(\sum_{\alpha_1^l \not\sim_U \alpha_1^m} \|\nu_l - T^{[1],up}_{lm}\nu_m\|^2 + \sum_{\alpha_1^l \sim_U \alpha_1^m} \|\nu_l + T^{[1],up}_{lm}\nu_m\|^2 \right). \tag{16}$$

Therefore it is apparent that $\mathcal{L}_1^{c,up}$ is Hermitian and semi-definite positive.

Table 2. Schematic representation of the four configurations induced by the directionality of the edges incident to the same nodes, which are captured by the Higher-order Connection Laplacian $L_1^{c,down}$.

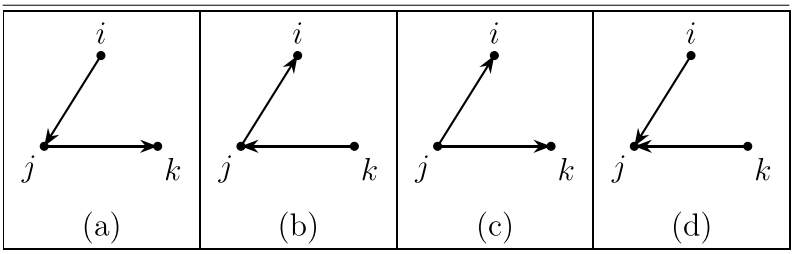

4.4. 1-down connection Laplacian

Now, let us define the 1-down connection Laplacian describing diffusion from edges to edges through vertices. To this end, we will follow a procedure similar to that employed in formulating the 1-up Connection Laplacian. However, there is an important difference. Since vertices have only one (trivial) possible direction, the number of configurations to consider is reduced to four instead of eight. These configurations are induced by the relative directions of the two edges, as illustrated in table 2. Another difference is that, in this case, the 1-down Hodge Laplacian of the undirected version of the simplicial complex and its Bochner matrix coincide. Therefore we first extract the diagonal and the off-diagonal entries of $\mathcal{L}_1^{down}$:

$$\mathcal{L}_1^{c,down} = D_1^{down} - A_1^{down}, \tag{17}$$

where

$$\left[A_1^{down}\right]_{lm} = \begin{cases} -1, & \text{if } \alpha_1^l \sim_L \alpha_1^m \\ 1, & \text{if } \alpha_1^l \not\sim_L \alpha_1^m \\ 0, & \text{otherwise,} \end{cases} \tag{18}$$

and D_1^{down} as the diagonal matrix of elements $[D_1^{down}]_{ll} = \sum_{m=1}^{n} |[A_1^{down}]_{lm}|$. Finally, the 1-down Connection Laplacian $\mathcal{L}_1^{c,down}$ is defined by incorporating information about edge orientation of the undirected version of the simplicial complex with A_1^{down} and the edge directions of the actual directed simplicial complex using a rotation matrix $T^{[1],down}$:

$$\mathcal{L}_1^{c,down} = D_1^{down} \otimes I_2 - T^{[1],down} \circ \left(A_1^{down} \otimes \mathbf{1}_2\right), \tag{19}$$

where for a constant $\delta \in [0, 2\pi)$ the 1-down rotation matrix $T^{[1],down}$ is given by

$$T^{[1],down}_{(ij),(jk)} = \begin{cases} e^{\mathbf{i}\delta}\boldsymbol{\sigma}_0, & \text{if } i \to j, j \to k \quad \text{(a)} \\ e^{-\mathbf{i}\delta}\boldsymbol{\sigma}_0, & \text{if } j \to i, k \to j \quad \text{(b)} \\ \boldsymbol{\sigma}_y, & \text{if } j \to i, j \to k \quad \text{(c)} \\ \boldsymbol{\sigma}_z, & \text{if } i \to j, k \to j \quad \text{(d)} \\ \boldsymbol{\sigma}_0, & \text{otherwise.} \end{cases} \tag{20}$$

Note that the letters in the above equation refer to the label of the configuration in table 2.

From this definition it can be easily shown that $\mathcal{L}_1^{c,down}$ is Hermitian as both D_1^{down} and A_1^{down} are real and symmetric; and $T^{[1],down}$ is Hermitian.

Assigning a complex vector $\nu_l \in \mathbb{C}^2$ to edge l, and let $\boldsymbol{\nu} = \{\nu_1, \ldots, \nu_n\}$, we have:

$$\boldsymbol{\nu}^\dagger \mathcal{L}_1^{c,down} \boldsymbol{\nu} = \frac{1}{2}\left(\sum_{\alpha_1^l \not\sim_L \alpha_1^m} \|\nu_l - T^{[1],down}_{lm} \nu_m\|^2 + \sum_{\alpha_1^l \sim_L \alpha_1^m} \|\nu_l + T^{[1],down}_{lm} \nu_m\|^2 \right). \tag{21}$$

Therefore we can conclude that $\mathcal{L}_1^{c,down}$ is positive semi-definite.

4.5. 2-down connection Laplacian for 2-dimensional orientable manifolds

The extension to Higher-order Connection Laplacians comes with additional challenges. For instance, in order to extend the above definition to the 2-down Connection Laplacian, relying solely on the definition of orientation and direction of triangles induced by the node labels is not sufficient to obtain Hermitian matrices. This implies that we cannot extend the above definition to treat the 2-down diffusion on a general simplicial complex. What we can do, however, is to consider simplicial complexes forming discrete orientable surfaces. For triangles, we can adopt the notion of orientation (and direction) induced by the orientation of the manifold. As for orientable continuous manifolds, for discrete orientable manifolds, we can distinguish two sides of a surface, with the normal vector to the manifold pointing either to one side or the other side of the manifold. The orientation of the manifold is determined by the choice of the normal vector direction. When considering $i,j,k \in V$ such that $[i,j,k]$ or any of its permutations form a 2-simplex, we represent its orientation as $\Delta_{ijk} = 1$ if, by following the right-hand rule and moving along the flow $i \to j \to k$ we obtain a vector pointing in the same direction as the normal vector to the manifold, otherwise we assign to the 2 simplex the orientation $\Delta_{ijk} = -1$.

In this way, it can be easily checked that the number of configurations induced by the relative directions of two triangles and their common edges is always eight as in the case in section 4.3. These configurations are shown schematically in figure 3. As for the 1-down Laplacian, also the 2-down Laplacian and its the Bochner matrices coincide. Therefore we first we extract the diagonal and the off-diagonal entries of $\mathcal{L}_2^{c,down}$:

$$\mathcal{L}_2^{c,down} = D_2^{down} - A_2^{down}, \tag{22}$$

where

$$\left[A_2^{down}\right]_{lm} = \begin{cases} -1, & \text{if } \alpha_2^l \sim_L \alpha_2^m \\ 1, & \text{if } \alpha_2^l \not\sim_L \alpha_2^m \\ 0, & \text{otherwise.} \end{cases} \tag{23}$$

and D_2^{down} as the diagonal matrix of non zero elements $[D_2^{down}]_{ll} = \sum_{m=1}^{n} |[A_2^{down}]_{lm}|$. Finally, the 2-down Connection Laplacian $\mathcal{L}_1^{c,down}$ is defined by incorporating both the triangle directions A_2^{down} and the edge directions using a rotation matrix $T^{[2],down}$:

$$\mathcal{L}_2^{c,down} = D_2^{down} \otimes I_2 - T^{[2],down} \circ \left(A_2^{down} \otimes \mathbf{1}_2\right), \tag{24}$$

where, considering rotations induced by the four Pauli matrices and the complex phase, we have

$$T^{[2],down}_{(ijk),(jkk')} = \begin{cases} e^{-\mathbf{i}\delta}\boldsymbol{\sigma}_0, & \text{if } \Delta_{ijk} = 1, \quad \Delta_{kjk'} = -1, \quad j \to k \quad \text{(a)} \\ e^{\mathbf{i}\delta}\boldsymbol{\sigma}_0, & \text{if } \Delta_{ijk} = -1, \quad \Delta_{kjk'} = 1, \quad k \to j \quad \text{(b)} \\ e^{-\mathbf{i}\delta}\boldsymbol{\sigma}_x, & \text{if } \Delta_{ijk} = -1, \quad \Delta_{kjk'} = 1, \quad j \to k \quad \text{(c)} \\ e^{\mathbf{i}\delta}\boldsymbol{\sigma}_x, & \text{if } \Delta_{ijk} = 1, \quad \Delta_{kjk'} = -1, \quad k \to j \quad \text{(d)} \\ e^{-\mathbf{i}\delta}\boldsymbol{\sigma}_y, & \text{if } \Delta_{ijk} = 1, \quad \Delta_{kjk'} = 1, \quad j \to k \quad \text{(e)} \\ e^{\mathbf{i}\delta}\boldsymbol{\sigma}_y, & \text{if } \Delta_{ijk} = 1, \quad \Delta_{kjk'} = 1, \quad k \to j \quad \text{(f)} \\ e^{-\mathbf{i}\delta}\boldsymbol{\sigma}_z, & \text{if } \Delta_{ijk} = -1, \quad \Delta_{kjk'} = -1, \quad j \to k \quad \text{(g)} \\ e^{\mathbf{i}\delta}\boldsymbol{\sigma}_z, & \text{if } \Delta_{ijk} = -1, \quad \Delta_{kjk'} = -1, \quad k \to j \quad \text{(h)} \\ \boldsymbol{\sigma}_0, & \text{otherwise,} \end{cases} \tag{25}$$

with the letters referring to the labels of the configurations in table 3. The associated quadratic form reads

$$\boldsymbol{\nu}^\dagger \mathcal{L}_2^{c,down} \boldsymbol{\nu} = \frac{1}{2} \left(\sum_{\alpha_2^l \not\sim_L \alpha_2^m} \|\nu_l - T^{[2],down}_{lm} \nu_m\|^2 + \sum_{\alpha_2^l \sim_L \alpha_2^m} \|\nu_l + T^{[2],down}_{lm} \nu_m\|^2 \right). \tag{26}$$

Note that the 2-down Connection Laplacian can be also extended to define the n-down Connection Laplacian of n-dimensional orientable manifolds, as the definition of this Connection Laplacian will always entail treating eight different configurations of relative directions of the two n-dimensional simplices and their incident $(n-1)$-dimensional simplex.

As we have seen, our formalism has allowed us to define the 0-up, the 1-up, the 1-down, and the 2-down Connection Laplacians of orientable, two-dimensional discrete manifolds. These operators allow us to distinguish between all possible configurations of the directions of the simplices by inducing rotations enforced through the matrices $T^{[n],up/down}$ leveraging on the use of the Pauli matrices, and a rotation of the phase in the complex plane.

Table 3. Schematic representation of the eight configurations induced by the directionality of two lower adjacent triangles and their common lower adjacent edge on 2-dimensional orientable manifolds. These configurations are captured by the Higher-order Connection Laplacian $L_{[2]}^{c,down}$.

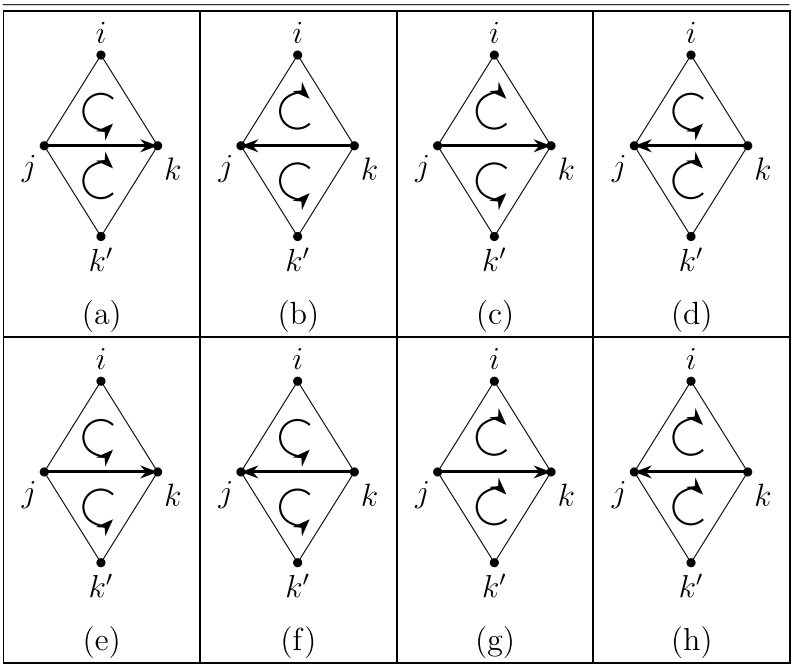

5. Higher-order diffusion on directed simplicial complexes

The Connection Laplacians defined in the previous section can be used to define higher-order diffusion processes that will reflect the directionality of the simplicial complex extending previous work on higher-order diffusion over undirected simplicial complexes [35–38]. If we focus on the diffusion induced by the 1-Connection Laplacian we can define three types of dynamical processes describing diffusion from edge to edge going exclusively through triangles (upper diffusion), going exclusively through nodes (lower diffusion), or going either through triangles or nodes (combined diffusion). These three types of diffusion process describe the evolution of the $1-$ *cochain* $\boldsymbol{\nu}$ whose elements ν_l defined on each edge l are complex valued 2-dimensional vectors, i.e. $\nu_l \in \mathbb{C}^2$. Specifically, we define three different types of higher-order dynamics: the upper, lower, and combined diffusion. In upper diffusion dynamics the dynamics of the edge topological signal $\boldsymbol{\nu} = \boldsymbol{\nu}(t)$ is driven by the process

$$\frac{\mathrm{d}\boldsymbol{\nu}(t)}{\mathrm{d}t} = -\mathcal{L}_1^{c,up}\boldsymbol{\nu}(t)\,. \tag{27}$$

Similarly, when the edge topological signal $\boldsymbol{\nu} = \boldsymbol{\nu}(t)$ follows the lower diffusion dynamics it obeys

$$\frac{\mathrm{d}\boldsymbol{\nu}(t)}{\mathrm{d}t} = -\mathcal{L}_1^{c,down}\boldsymbol{\nu}(t)\,, \tag{28}$$

Finally if the edge topological signal $\boldsymbol{\nu} = \boldsymbol{\nu}(t)$ follows combined diffusion, then it will evolve according to

$$\frac{\mathrm{d}\boldsymbol{\nu}(t)}{\mathrm{d}t} = -\left(\mathcal{L}_1^{c,up} + \mathcal{L}_1^{c,down}\right)\boldsymbol{\nu}(t)\,. \tag{29}$$

Note that since in general $\mathcal{L}_1^{c,up}$ and $\mathcal{L}_1^{c,down}$ do not obey Hodge decomposition, the combined diffusion process cannot be easily recast into the upper and the lower diffusion dynamics as happens in diffusion determined by the Hodge Laplacian in undirected simplicial complexes [35, 89].

The properties of the higher-order diffusion (of order 1) on directed simplicial complexes will depend strongly on the structure of the simplicial complex and the directionality of the edges. Here we provide a discussion of these higher-order diffusion processes in different cases of directed triangles and on a directed torus. For each case considered, we will investigate the spectral properties of the 1-up and 1-down Connection Laplacians as a function of the parameter δ and we will computer the commutator

$$\left[\mathcal{L}_1^{c,up}, \mathcal{L}_1^{c,down}\right] = \mathcal{L}_1^{c,up}\mathcal{L}_1^{c,down} - \mathcal{L}_1^{c,down}\mathcal{L}_1^{c,up}. \tag{30}$$

Table 4. Schematic representation of the 4 distinct types of 2-dimensional directed simplicial complexes formed by one directed triangles, three directed edges and three vertices.

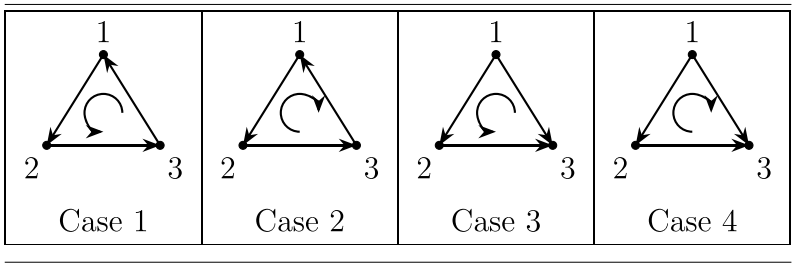

While in this paper we mostly focus on these three types of topological diffusion, that define a classical dynamics, our results on the spectral properties of the Higher-order Connection Laplacian can be applied as well to the following three distinct types of Schrödinger equations: the upper, the lower and the combined Schrödinger equations. The upper-Schrödinger equation is driven by the upper Higher-Order Connection Laplacian

$$\mathrm{i}\frac{\mathrm{d}\boldsymbol{\nu}(t)}{\mathrm{d}t} = \mathcal{L}_1^{c,up}\boldsymbol{\nu}(t)\,, \tag{31}$$

the lower-Schröedinger equation is driven by the lower Higher-Order Connection Laplacian,

$$\mathrm{i}\frac{\mathrm{d}\boldsymbol{\nu}(t)}{\mathrm{d}t} = \mathcal{L}_1^{c,down}\boldsymbol{\nu}(t)\,, \tag{32}$$

and the combined Schröedinger equation is driven by the sum of the upper and the lower Higher-Order Connection Laplacian, i.e.

$$\mathrm{i}\frac{\mathrm{d}\boldsymbol{\nu}(t)}{\mathrm{d}t} = \left(\mathcal{L}_1^{c,up} + \mathcal{L}_1^{c,down}\right)\boldsymbol{\nu}(t)\,. \tag{33}$$

In main difference between the classical (topological) dynamics that we describe here in detail and these Schrödinger equations is that the diffusion dynamics will always relax to the fundamental state, while the quantum evolution will consist of sustained oscillations. This sustained oscillations include different modes corresponding to the different eigenvectors of the Higher-order Connection Laplacian, each one oscillating at a frequency $\omega = \lambda$ where λ is their associated eigenvalue and $E = \omega$ their associated energy.

5.1. Directed simplicial triangles

Let us now explore some examples of directed triangles formed by three vertices $[1], [2], [3]$, three edges $[1,2]$, $[1,3]$, $[2,3]$, and one triangle $[1,2,3]$, where the edges and the triangles have a given direction, leading to the four distinct scenarios depicted in table 4. In addition to analysing of the spectral properties of these simplicial triangles, for each considered case, we will also analyse the quadratic form of the Higher-order Connection Laplacians and determine conditions under which it can be minimized to zero. Finally, we will provide a numerical investigation of the dynamical properties of the induced higher-order diffusion processes.

5.1.1. Case 1

We consider the directed 2-simplicial complex denoted as Case 1 in table 4, having edge directions given by $1 \to 2$, $2 \to 3$, and $3 \to 1$; and triangle direction $1 \to 2 \to 3$. This represents the scenario where all edge directions conform to the direction of the triangle. Hence, if we traverse from one edge to another, we either align with both the directions of the edge and the triangle, as shown in the first row of (14); or we go against both the edge and triangle directions, corresponding to the second row in (14). For the 1-up Connection Laplacian, we obtain the following:

$$\mathcal{L}_1^{c,up} = \begin{matrix}[1,2]\\[1,3]\\[2,3]\end{matrix}\begin{pmatrix} \begin{matrix}[1,2]\\ 2\boldsymbol{\sigma}_0\end{matrix} & \begin{matrix}[1,3]\\ -\boldsymbol{\sigma}_y e^{\mathbf{i}\delta}\end{matrix} & \begin{matrix}[2,3]\\ \boldsymbol{\sigma}_0 e^{-\mathbf{i}\delta}\end{matrix} \\ -\boldsymbol{\sigma}_y e^{-\mathbf{i}\delta} & 2\boldsymbol{\sigma}_0 & -\boldsymbol{\sigma}_z e^{\mathbf{i}\delta} \\ \boldsymbol{\sigma}_0 e^{\mathbf{i}\delta} & -\boldsymbol{\sigma}_z e^{-\mathbf{i}\delta} & 2\boldsymbol{\sigma}_0 \end{pmatrix}. \tag{34}$$

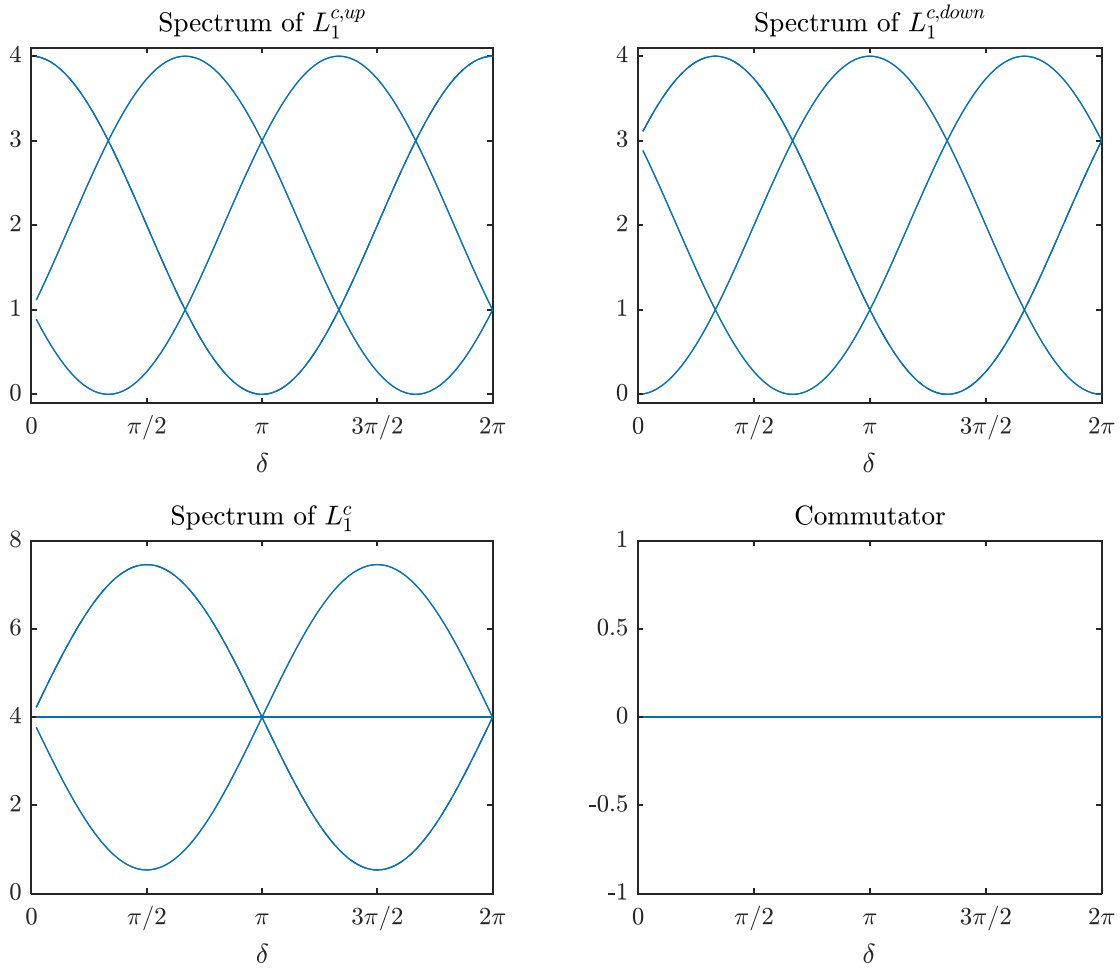

Figure 2. The complete spectrum of $\mathcal{L}_1^{c,up}$ (top-left), $\mathcal{L}_1^{c,down}$ (top-right), and $\mathcal{L}_1^{c}$ (bottom-left), and commutator $[\mathcal{L}_1^{c,up}, \mathcal{L}_1^{c,down}]$ (bottom-right) for Case 1 directed simplicial triangles is plotted as a function of δ.

In the top left panel of figure 2, we display the eigenvalues of $\mathcal{L}_1^{c,up}$ in relation to δ. The corresponding eigenvalues are:

$$\{2+2\cos(\delta), 2+2\cos(\delta-2\pi/3), 2+2\cos(\delta-4\pi/3)\}. \tag{35}$$

To compute the quadratic form, we denote the components of the 1-cochain as $\boldsymbol{\nu}\,\boldsymbol{\nu} = (\nu_1,\nu_2,\nu_3)' \in \mathbb{C}^6$ corresponding to the three edges $[1,2]$, $[1,3]$, and $[2,3]$ respectively. Here and in the following we parameterize each component ν_l of the 1-cochain with three angles (θ_l,ϕ_l and ψ_l) by setting

$$\nu_l = \left(\cos(\psi_l)\, e^{\mathbf{i}\theta_l}, \sin(\psi_l)\, e^{\mathbf{i}\phi_l}\right)' \in \mathbb{C}^2, \tag{36}$$

where $\psi_l \in [0, \frac{\pi}{2}]$, and $\theta_l, \phi_l \in [0, 2\pi)$. Therefore the 1-up Connection Laplacian is associated to the quadratic form

$$\boldsymbol{\nu}^H \mathcal{L}_1^{c,up} \boldsymbol{\nu} = \|\nu_1 - \boldsymbol{\sigma}_0 e^{\mathbf{i}\delta}\nu_2\|^2 + \|\nu_1 + \boldsymbol{\sigma}_0 e^{-\mathbf{i}\delta}\nu_3\|^2 + \|\nu_2 - \boldsymbol{\sigma}_0 e^{\mathbf{i}\delta}\nu_3\|^2. \tag{37}$$

The quadratic form above equals zero when $\psi_1 = \psi_2 = \psi_3$, and

$$\theta_1 \equiv \theta_2 + \delta,\ \phi_1 \equiv \phi_2 + \delta, \tag{38}$$

$$\theta_1 \equiv \theta_3 - \delta + \pi\,,\ \phi_1 \equiv \phi_3 - \delta + \pi\,, \tag{39}$$

$$\theta_2 \equiv \theta_3 + \delta,\ \phi_2 \equiv \phi_3 + \delta. \tag{40}$$

A solution exists only when $\delta = \pi/3, \pi$, or $5\pi/3$, as shown in the top-left panel of figure 2. When δ takes the aforementioned values, $\boldsymbol{\nu}$, which satisfy the above conditions, becomes an eigenvector of $\mathcal{L}_1^{c,up}$ associated with an eigenvalue of zero.

For the 1-down Connection Laplacian, we have

$$\mathcal{L}_1^{c,down} = \begin{matrix}[1,2]\\[1,3]\\[2,3]\end{matrix} \begin{matrix}\begin{matrix}[1,2] & [1,3] & [2,3]\end{matrix}\\ \begin{pmatrix} 2\boldsymbol{\sigma}_0 & \boldsymbol{\sigma}_0 e^{-\mathbf{i}\delta} & -\boldsymbol{\sigma}_0 e^{\mathbf{i}\delta} \\ \boldsymbol{\sigma}_0 e^{\mathbf{i}\delta} & 2\boldsymbol{\sigma}_0 & \boldsymbol{\sigma}_0 e^{-\mathbf{i}\delta} \\ -\boldsymbol{\sigma}_0 e^{-\mathbf{i}\delta} & \boldsymbol{\sigma}_0 e^{\mathbf{i}\delta} & 2\boldsymbol{\sigma}_0 \end{pmatrix}\end{matrix}. \tag{41}$$

Eigenvalues of $\mathcal{L}_1^{c,down}$, as shown in the top-right plot in figure 2, are:

$$\{2-2\cos(\delta+\pi/3), 2-2\cos(\delta), 2-2\cos(\delta-\pi/3)\}. \tag{42}$$

The corresponding quadratic form of the 1-down Connection Laplacians are

$$\boldsymbol{\nu}^H \mathcal{L}_1^{c,down} \boldsymbol{\nu} = \|\nu_1 + \boldsymbol{\sigma}_0 e^{-\mathbf{i}\delta}\nu_2\|^2 + \|\nu_1 - \boldsymbol{\sigma}_0 e^{\mathbf{i}\delta}\nu_3\|^2 + \|\nu_2 + \boldsymbol{\sigma}_0 e^{-\mathbf{i}\delta}\nu_3\|^2. \tag{43}$$

It becomes zero when $\psi_1 = \psi_2 = \psi_3$, and

$$\theta_1 \equiv \theta_2 - \delta + \pi, \phi_1 \equiv \phi_2 - \delta + \pi, \tag{44}$$
$$\theta_1 \equiv \theta_3 - \delta + \pi, \phi_1 \equiv \phi_3 + \delta, \tag{45}$$
$$\theta_2 \equiv \theta_3 - \delta + \pi, \phi_2 \equiv \phi_3 - \delta + \pi. \tag{46}$$

A solution exists only when $\delta = 0, 2\pi/3$, or $4\pi/3$, as shown in the top-right panel in figure 2.

Upon combining the 1-up and 1-down Connection Laplacians, we obtain the eigenvalues of their sum, as depicted in the bottom-left panel of figure 2. The corresponding eigenvalues are

$$\left\{3, 3+2\sqrt{3}\sin(\delta), 3-2\sqrt{3}\sin(\delta)\right\}. \tag{47}$$

The 1-up and the 1-down Connection Laplacians $\mathcal{L}_1^{c,up}$ and $\mathcal{L}_1^{c,down}$ commute since the commutator is zero (bottom-right panel in figure 2). Furthermore, it can be shown that $\mathcal{L}_1^{c,down}\mathcal{L}_1^{c,up} \neq 0$, which implies that the Hodge decomposition does not hold, i.e. $\mathcal{L}_1^{c,up}\mathcal{L}_1^{c,down} \neq 0, \mathcal{L}_1^{c,down}\mathcal{L}_1^{c,up} \neq 0$ for all values of δ.

Figure 3 plots two examples when the dynamics are described by $\mathcal{L}_1^{c,up}$ (left), $\mathcal{L}_1^{c,down}$ (middle), and their sum (right) for various value of δ. For visualization purposes, we only display the phase angles. Setting $\delta = \pi/3$ (figure 3(a)) and examining the plot for $\mathcal{L}_1^{c,up}$, we notice that it converges towards an eigenvector of $\mathcal{L}_1^{c,up}$ associated with an eigenvalue of zero, which satisfies conditions (39) and (40). Since $\mathcal{L}_1^{c,\text{down}}$ and $\mathcal{L}_1^{c,\text{up}} + \mathcal{L}_1^{c,\text{down}}$ only possess positive eigenvalues when $\delta = \pi/3$, the vectors converge into their slow eigenmodes associated with the smallest eigenvalue. We observe similar results when $\delta = 2\pi/3$ (figure 3(b)), where the equilibrium vector is an eigenvector of $\mathcal{L}_1^{c,down}$ corresponding to the 0 eigenvalue satisfying (44)–(46).

5.1.2. Case 2

Now, let us consider Case 2 in table 4, where the edge directions are as follows: $1 \to 2$, $2 \to 3$, and $3 \to 1$; and the triangle direction is $3 \to 2 \to 2 \to 1$. This scenario represents a situation where all edge directions are opposite to the direction of the triangle. Consequently, when traversing from one edge to another, we either move against the edge direction while aligning with the triangle direction—as shown in the third row of (14)—or align with the edge direction while moving against the triangle direction, as depicted in the fourth row of (14). The corresponding 1-up Connection Laplacian is

$$\mathcal{L}_1^{c,up} = \begin{matrix}[1,2]\\[1,3]\\[2,3]\end{matrix} \begin{matrix}\begin{matrix}[1,2] & [1,3] & [2,3]\end{matrix}\\ \begin{pmatrix} 2\boldsymbol{\sigma}_0 & -\boldsymbol{\sigma}_x e^{-\mathbf{i}\delta} & \boldsymbol{\sigma}_x e^{\mathbf{i}\delta} \\ -\boldsymbol{\sigma}_x e^{\mathbf{i}\delta} & 2\boldsymbol{\sigma}_0 & -\boldsymbol{\sigma}_x e^{-\mathbf{i}\delta} \\ \boldsymbol{\sigma}_x e^{-\mathbf{i}\delta} & -\boldsymbol{\sigma}_x e^{\mathbf{i}\delta} & 2\boldsymbol{\sigma}_0 \end{pmatrix}\end{matrix}. \tag{48}$$

Then the quadratic form $\boldsymbol{\nu}^H \mathcal{L}_1^{c,up} \boldsymbol{\nu}$ can be calculated as

$$\boldsymbol{\nu}^H \mathcal{L}_1^{c,up} \boldsymbol{\nu} = \|\nu_1 - \boldsymbol{\sigma}_x e^{-\mathbf{i}\delta}\nu_2\|^2 + \|\nu_1 + \boldsymbol{\sigma}_x e^{\mathbf{i}\delta}\nu_3\|^2 + \|\nu_2 - \boldsymbol{\sigma}_x e^{-\mathbf{i}\delta}\nu_3\|^2. \tag{49}$$

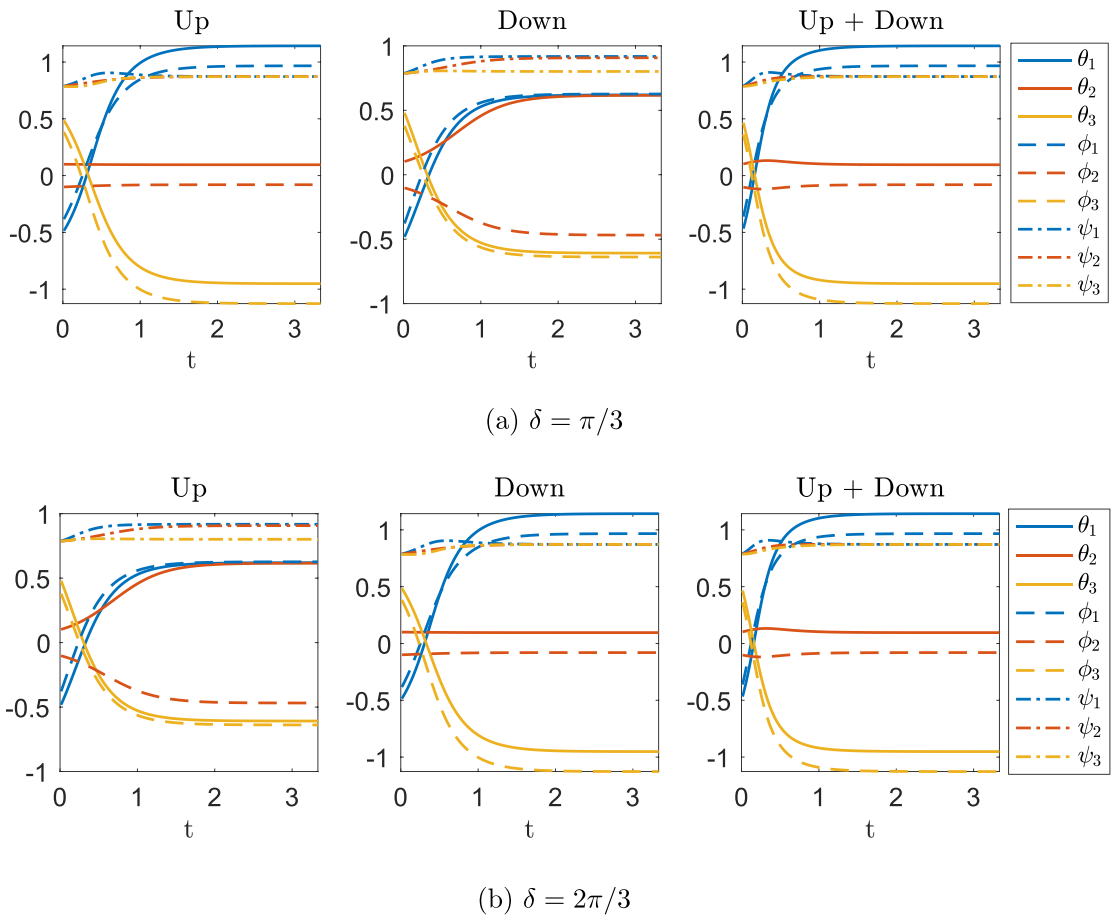

Figure 3. Higher-order diffusion driven by the 1-Connection Laplacians $\mathcal{L}_1^{up}$ (Up), $\mathcal{L}_1^{down}$ (Down) and $\mathcal{L}_1$ (Up+Down) on directed simplicial triangle in Case 1 are plotted for single initial conditions and for $\delta = \pi/3$ (upper row) and $\delta = 2\pi/3$ (lower row). In the upper-left plot, the final state is an eigenvector of $\mathcal{L}_1^{c,up}$ corresponding to the 0 eigenvalue, while in the lower-middle plot, the equilibrium vector is an eigenvector of $\mathcal{L}_1^{c,down}$ corresponding to the 0 eigenvalue. In the remaining plots, the final states converge to the slowest eigenmodes associated with the smallest positive eigenvalue.

We plot its eigenvalues against δ in the top left panel of figure (2). The corresponding eigenvalues are:

$$\left\{2+2\cos(\delta), 2+2\cos\left(\delta-\frac{\pi}{3}\right), 2+2\cos\left(\delta-\frac{2\pi}{3}\right), 2+2\cos(\delta-\pi),\right.$$
$$\left. 2+2\cos\left(\delta-\frac{4\pi}{3}\right), 2+2\cos\left(\delta-\frac{5\pi}{3}\right)\right\}. \tag{50}$$

It may be shown that $\boldsymbol{\nu}^H \mathcal{L}_1^{c,up} \boldsymbol{\nu} = 0$ when $\psi_1 = \psi_2 = \psi_3 = \pi/4$, and

$$\theta_1 \equiv \phi_2 - \delta,\ \phi_1 \equiv \theta_2 - \delta, \tag{51}$$
$$\theta_1 \equiv \phi_3 + \delta + \pi,\ \phi_1 \equiv \theta_3 + \delta + \pi, \tag{52}$$
$$\theta_2 \equiv \phi_3 - \delta,\ \phi_2 \equiv \theta_3 - \delta. \tag{53}$$

The equations above have a solution only when $\delta \in \{0, \pi/3, 2\pi/3, \pi, 4\pi/3, 5\pi/3\}$, as can be seen in the plot. In Case 2, $\mathcal{L}_1^{c,down}$ remains the same as in Case 1 since the edge directions stay unchanged. The eigenvalues of $\mathcal{L}_1^{c,up} + \mathcal{L}_1^{c,down}$ are

$$\left\{4+4\cos\left(\delta-\frac{\pi}{3}\right), 4+4\cos(\delta-\pi), 4+4\cos\left(\delta-\frac{5\pi}{3}\right), 4\right\}. \tag{54}$$

The commutator $[\mathcal{L}_1^{c,down}, \mathcal{L}_1^{c,up}]$ is zero, i.e. $[\mathcal{L}_1^{c,down}, \mathcal{L}_1^{c,up}] = 0$, as shown in the bottom-right of figure 4, however Hodge decomposition does not hold as in Case 1. Figure 5 displays two examples of vector diffusion. When $\delta = \pi/3$, the vectors in the left plot converge toward an eigenvector of $\mathcal{L}_1^{c,up}$ corresponding to eigenvalue zero, satisfying conditions (51)–(53). When $\delta = 2\pi/3$, the equilibrium vector for both $\mathcal{L}_1^{c,up}$ (on the left) and $\mathcal{L}_1^{c,down}$ (in the middle) are eigenvectors associated with a zero eigenvalue, as specified by

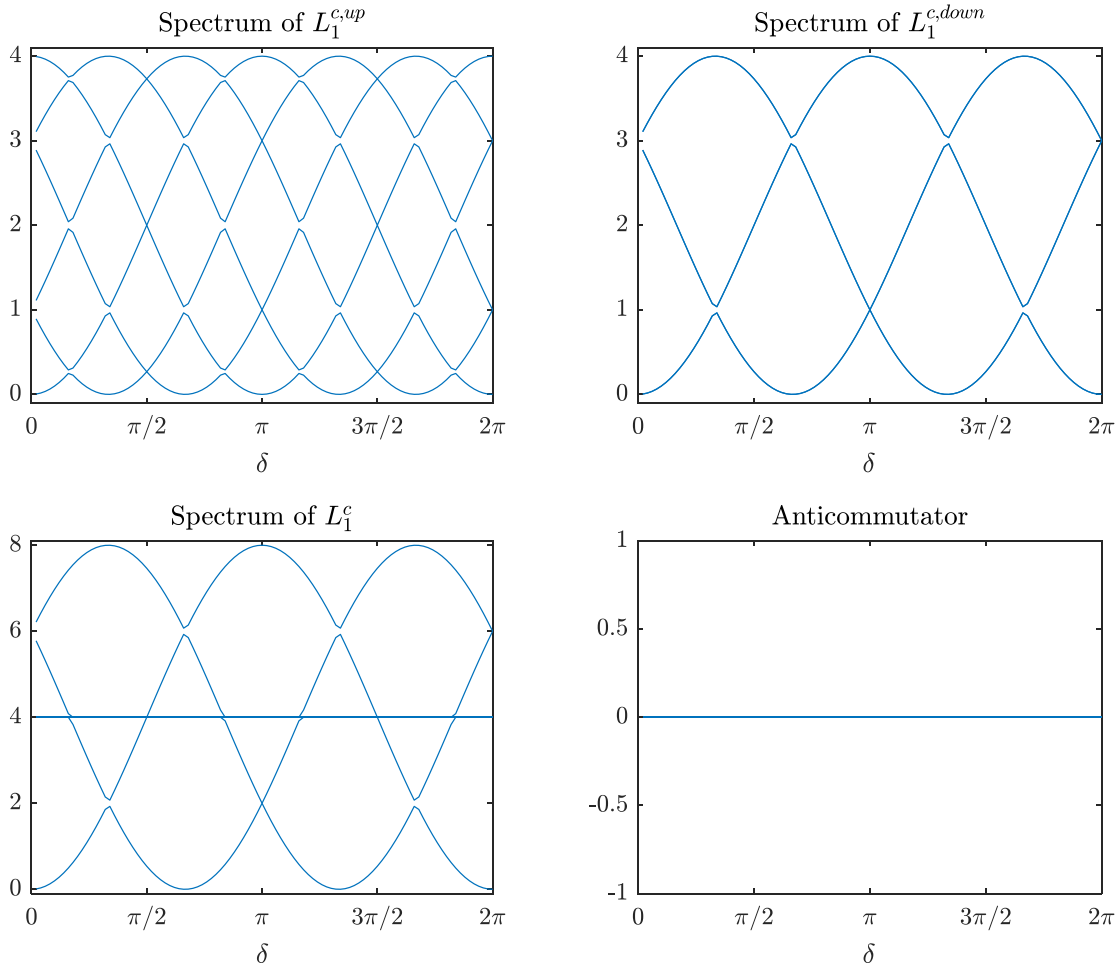

Figure 4. The complete spectra of $\mathcal{L}_1^{c,up}$ (top-left), $\mathcal{L}_1^{c,down}$ (top-right), and $\mathcal{L}_1^c$ (bottom-left), and commutator $[\mathcal{L}_1^{c,up}, \mathcal{L}_1^{c,down}]$ (bottom-right) for Case 2 directed simplicial triangles is plotted as a function of δ.

conditions (51)–(53) and (44)–(46) respectively. In the remaining plots, the final states converge toward the slowest eigenmodes associated with the smallest positive eigenvalue due to the absence of a zero eigenvalue.

5.1.3. Case 3

Now, let us look at the case of a 2-simplicial complex with triangle and link direction given by $1 \to 2 \to 3$ and $1 \to 2$, $2 \to 3$ and $1 \to 3$, which is illustrated as Case 3 in table 4. First, we can write the 1-up and 1-down Connection Laplacian as

$$\mathcal{L}_1^{c,up} = \begin{matrix}[1,2]\\[1,3]\\[2,3]\end{matrix} \begin{pmatrix} \begin{matrix}[1,2]\end{matrix} & \begin{matrix}[1,3]\end{matrix} & \begin{matrix}[2,3]\end{matrix} \\ 2\boldsymbol{\sigma}_0 & -\boldsymbol{\sigma}_y e^{\mathbf{i}\delta} & \boldsymbol{\sigma}_0 e^{-\mathbf{i}\delta} \\ -\boldsymbol{\sigma}_y e^{-\mathbf{i}\delta} & 2\boldsymbol{\sigma}_0 & -\boldsymbol{\sigma}_z e^{\mathbf{i}\delta} \\ \boldsymbol{\sigma}_0 e^{\mathbf{i}\delta} & -\boldsymbol{\sigma}_z e^{-\mathbf{i}\delta} & 2\boldsymbol{\sigma}_0 \end{pmatrix}. \tag{55}$$

Its quadratic form is

$$\boldsymbol{\nu}^H \mathcal{L}_1^{c,up} \boldsymbol{\nu} = \|\nu_1 - \boldsymbol{\sigma}_y e^{\mathbf{i}\delta} \nu_2\|^2 + \|\nu_1 + \boldsymbol{\sigma}_0 e^{-\mathbf{i}\delta} \nu_3\|^2 + \|\nu_2 - \boldsymbol{\sigma}_z e^{\mathbf{i}\delta} \nu_3\|^2, \tag{56}$$

and it becomes zero when $\psi_1 = \psi_2 = \psi_3 = \pi/4$ and

$$\theta_1 \equiv \phi_2 + \delta - \frac{\pi}{2}, \phi_1 \equiv \theta_2 + \delta + \frac{\pi}{2}, \tag{57}$$

$$\theta_1 \equiv \theta_3 - \delta + \pi, \phi_1 \equiv \phi_3 - \delta + \pi, \tag{58}$$

$$\theta_2 \equiv \phi_3 + \delta, \phi_2 \equiv \phi_3 + \delta + \pi. \tag{59}$$

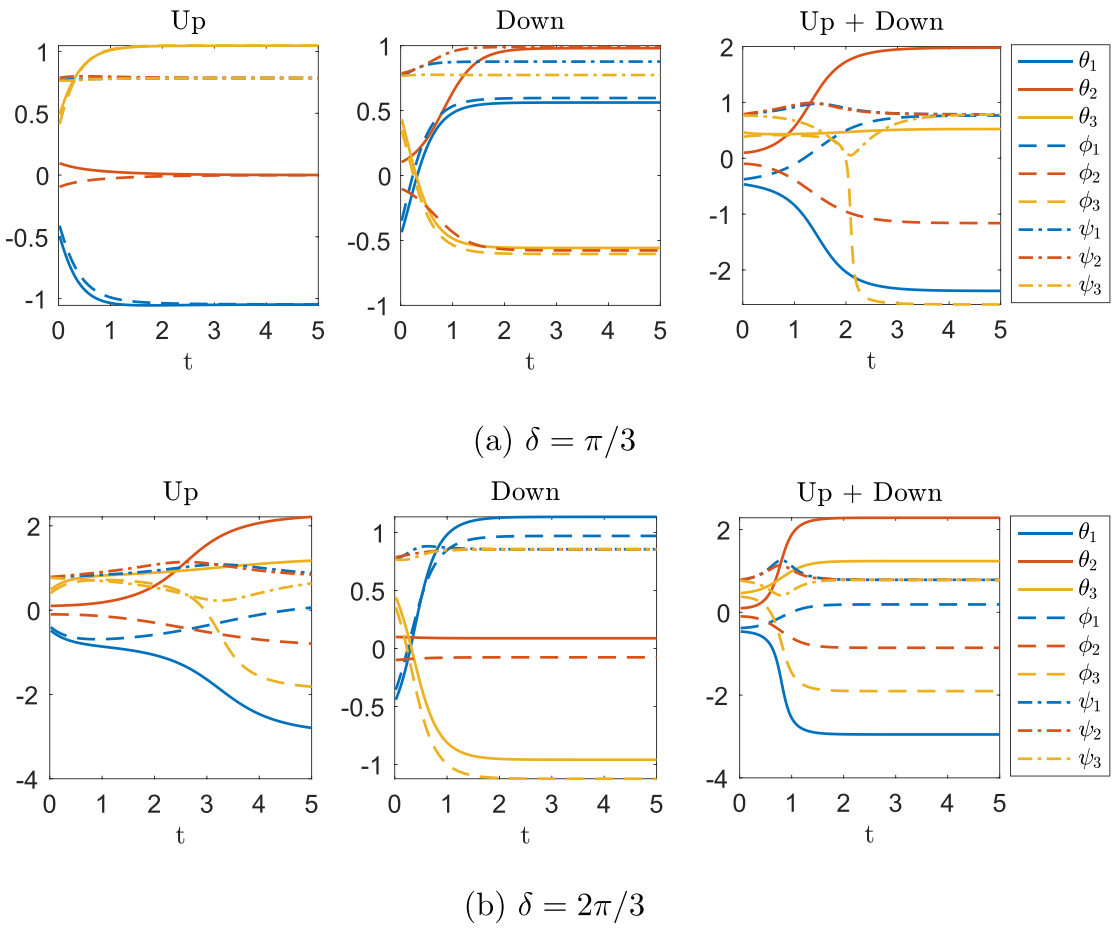

Figure 5. Higher-order diffusion driven by the 1-Connection Laplacians $\mathcal{L}_1^{up}$ (Up), $\mathcal{L}_1^{down}$ (Down) and $\mathcal{L}_1$ (Up+Down) on directed simplicial triangle in Case 2 are plotted for single initial conditions and for $\delta = \pi/3$ (upper row) and $\delta = 2\pi/3$ (lower row). In the upper-left plot, vectors converge towards an eigenvector of $\mathcal{L}_1^{c,up}$ with an eigenvalue of zero. In the lower plot, where $\delta = 2\pi/3$, both equilibrium vectors for $\mathcal{L}_1^{c,up}$ (on the left) and $\mathcal{L}_1^{c,down}$ (in the middle) are eigenvectors associated with a zero eigenvalue. Across the remaining plots, the final states converge to the slowest eigenmodes linked to the smallest positive eigenvalue due to the absence of a zero eigenvalue.

The above system has a solution iff $\delta \in \{\pi/6, \pi/2, 5\pi/6, 7\pi/6, 3\pi/2, 11\pi/6\}$. This can be confirmed by the eigenvalue top-left plot in figure 6. Furthermore, the eigenvalues are given by

$$\begin{aligned}&\left\{2+2\cos\left(\delta-\tfrac{\pi}{6}\right), 2+2\cos\left(\delta-\tfrac{\pi}{2}\right),\right.\\ &2+2\cos\left(\delta-\tfrac{5\pi}{6}\right), 2+2\cos\left(\delta-\tfrac{7\pi}{6}\right),\\ &\left.2+2\cos\left(\delta-\tfrac{3\pi}{2}\right), 2+2\cos\left(\delta-\tfrac{11\pi}{6}\right)\right\}.\end{aligned} \tag{60}$$

For the 1-down Connection Laplacian, we have

$$\mathcal{L}_1^{c,down} = \begin{matrix}\\ [1,2]\\ [1,3]\\ [2,3]\end{matrix}\begin{matrix}\begin{matrix}[1,2] & [1,3] & [2,3]\end{matrix}\\ \begin{pmatrix} 2\sigma_0 & \boldsymbol{\sigma}_y & -\boldsymbol{\sigma}_0 e^{\mathbf{i}\delta} \\ \boldsymbol{\sigma}_y & 2\boldsymbol{\sigma}_0 & \boldsymbol{\sigma}_z \\ -\boldsymbol{\sigma}_0 e^{-\mathbf{i}\delta} & \boldsymbol{\sigma}_z & 2\boldsymbol{\sigma}_0 \end{pmatrix}\end{matrix}, \tag{61}$$

and

$$\boldsymbol{\nu}^H \mathcal{L}_1^{c,down} \boldsymbol{\nu} = \|\nu_1 + \boldsymbol{\sigma}_y \nu_2\|^2 + \|\nu_1 - \boldsymbol{\sigma}_0 e^{\mathbf{i}\delta} \nu_3\|^2 + \|\nu_2 + \boldsymbol{\sigma}_z \nu_3\|^2. \tag{62}$$

The quadratic form is zero when $\psi_1 = \psi_2 = \psi_3 = \pi/4$ and

$$\theta_1 \equiv \phi_2 + \frac{\pi}{2}, \phi_1 \equiv \theta_2 - \frac{\pi}{2}, \tag{63}$$

$$\theta_1 \equiv \theta_3 + \delta, \phi_1 \equiv \phi_3 + \delta, \tag{64}$$

$$\theta_2 \equiv \theta_3 + \pi, \phi_2 \equiv \phi_3. \tag{65}$$

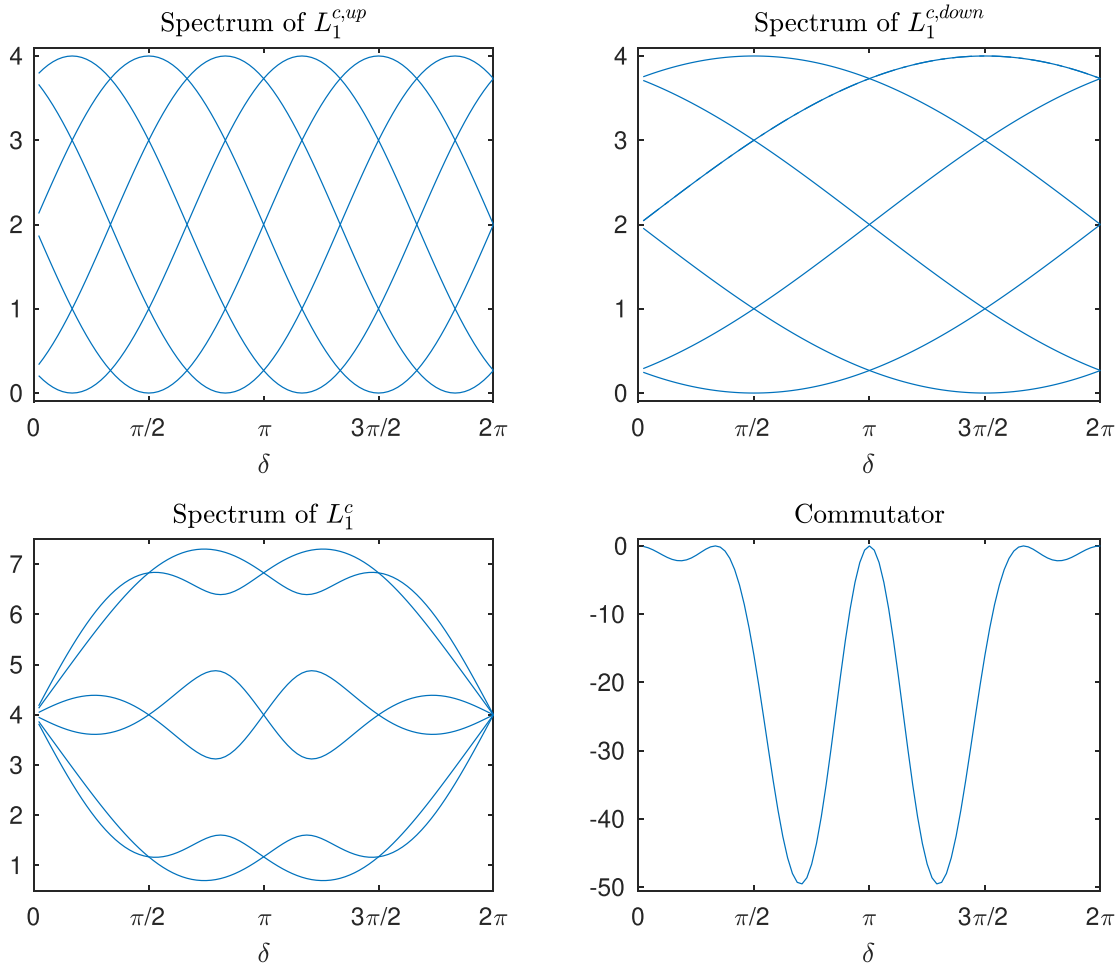

Figure 6. The complete spectra of 1-Connection Laplacians $\mathcal{L}_1^{c,up}$ (top-left), $\mathcal{L}_1^{c,down}$ (top-right), and $\mathcal{L}_1^{c}$ (bottom-left), and commutator $[\mathcal{L}_1^{c,up}, \mathcal{L}_1^{c,down}]$(bottom-right) for Case 3 directed simplicial triangles is plotted as a function of δ.

The equation above can be solved iff $\delta \in \{\pi/2, 3\pi/2\}$ as shown in the top-right plot in figure 6. Furthermore, the eigenvalues are given by

$$\begin{aligned}&\left\{2+2\cos\left(\frac{\delta}{3}-\frac{\pi}{6}\right), 2-2\cos\left(\frac{\delta}{3}-\frac{\pi}{6}\right),\right.\\ &2+2\cos\left(\frac{\delta}{3}-\frac{\pi}{2}\right), 2-2\cos\left(\frac{\delta}{3}-\frac{\pi}{2}\right),\\ &\left.2+2\cos\left(\frac{\delta}{3}-\frac{5\pi}{6}\right), 2-2\cos\left(\frac{\delta}{3}-\frac{5\pi}{6}\right)\right\}.\end{aligned} \tag{66}$$

In this case $\mathcal{L}_1^{c,up}$ and $\mathcal{L}_1^{c,up}$ do not commute except for the special case when $\delta = 0$ as shown in the bottom-right panel in figure 6. Two examples of vector diffusion are displayed in figure 7 for $\delta = \pi/2$ and $3\pi/2$. In both scenarios, the vectors for $\mathcal{L}_1^{c,up}$ and $\mathcal{L}_1^{c,down}$, the vectors approach some eigenvectors that correspond to eigenvalue zero, which satisfies conditions (57)–(59) and (63)–(65) respectively.

5.1.4. Case 4

Finally, we examine the directed 2-simplicial complex with triangle and link direction given by $3 \to 2 \to 1$ and $1 \to 2$, $2 \to 3$ and $1 \to 3$ illustrated as Case 4 in figure 4. As the edge directions are precisely the same as in Case 3, $\mathcal{L}_1^{c,down}$ in this scenario is identical to the previous case. Therefore, we only need to discuss $\mathcal{L}_1^{c,up}$, which can be computed as follows:

$$\mathcal{L}_1^{c,up} = \begin{matrix}[1,2]\\[1,3]\\[2,3]\end{matrix}\begin{pmatrix} \begin{matrix}[1,2]\\ 2\boldsymbol{\sigma}_0\end{matrix} & \begin{matrix}[1,3]\\ -\boldsymbol{\sigma}_y e^{-\mathbf{i}\delta}\end{matrix} & \begin{matrix}[2,3]\\ \boldsymbol{\sigma}_x e^{\mathbf{i}\delta}\end{matrix} \\ -\boldsymbol{\sigma}_y e^{\mathbf{i}\delta} & 2\boldsymbol{\sigma}_0 & -\boldsymbol{\sigma}_z e^{-\mathbf{i}\delta} \\ \boldsymbol{\sigma}_x e^{-\mathbf{i}\delta} & -\boldsymbol{\sigma}_z e^{\mathbf{i}\delta} & 2\boldsymbol{\sigma}_0 \end{pmatrix}. \tag{67}$$

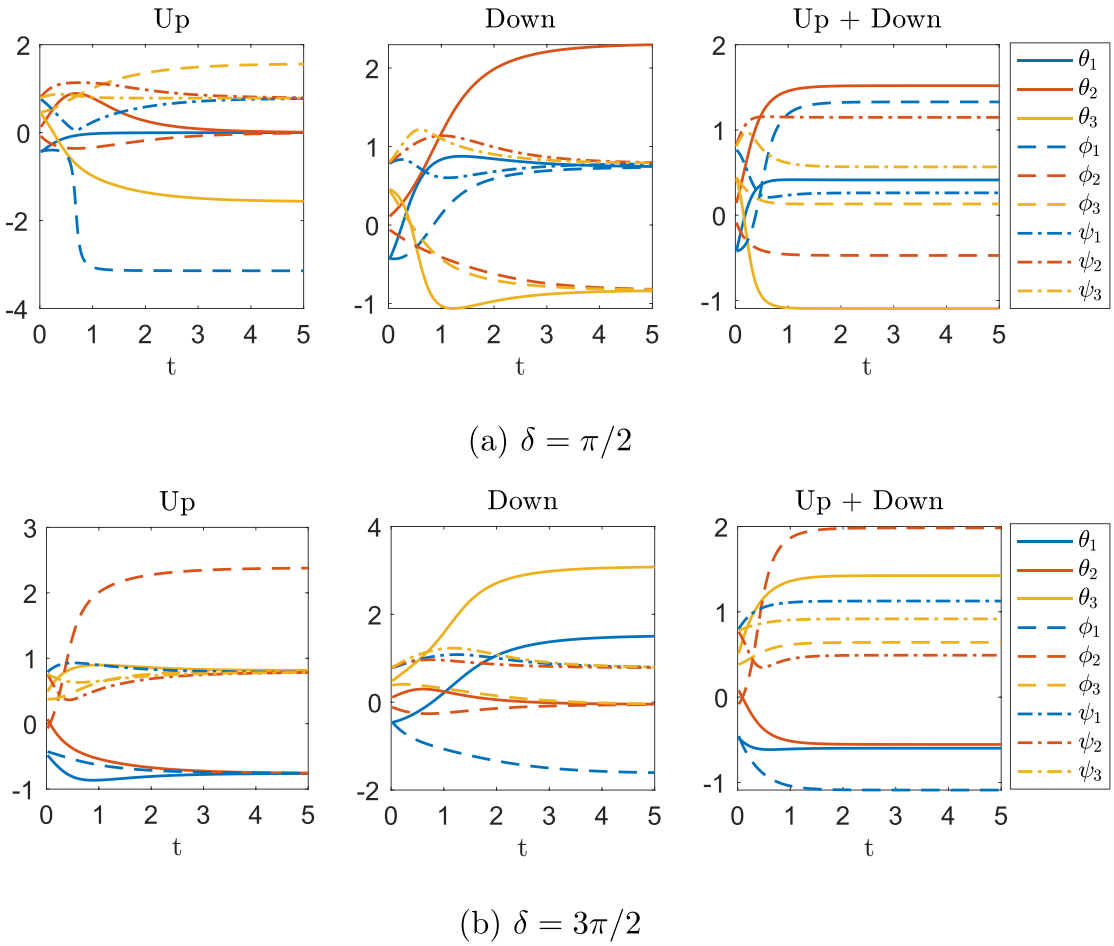

Figure 7. Higher-order diffusion driven by the 1-Connection Laplacians $\mathcal{L}_1^{up}$ (Up), $\mathcal{L}_1^{down}$ (Down) and $\mathcal{L}_1$ (Up+Down) on directed simplicial triangle in Case 3 are plotted for single initial conditions and for $\delta = \pi/3$ (upper row) and $\delta = 2\pi/3$ (lower row). In both situations, the vectors associated with $\mathcal{L}_1^{c,\text{up}}$ and $\mathcal{L}_1^{c,\text{down}}$ converge towards eigenvectors corresponding to a zero eigenvalue.

This leads to

$$\boldsymbol{\nu}^H \mathcal{L}_1^{c,up} \boldsymbol{\nu} = \|\nu_1 - \boldsymbol{\sigma}_y e^{-\mathbf{i}\delta} \nu_2\|^2 + \|\nu_1 + \boldsymbol{\sigma}_x e^{\mathbf{i}\delta} \nu_3\|^2 + \|\nu_2 - \boldsymbol{\sigma}_z e^{-\mathbf{i}\delta} \nu_3\|^2. \tag{68}$$

We can further prove that $\boldsymbol{\nu}^H \mathcal{L}_1^{c,up} \boldsymbol{\nu} = 0$ when $\pi/2 - \psi_1 = \psi_2 = \psi_3$, and

$$\theta_1 \equiv \phi_2 - \delta - \frac{\pi}{2}, \phi_1 \equiv \theta_2 - \delta + \frac{\pi}{2}, \tag{69}$$

$$\theta_1 \equiv \phi_3 + \delta + \pi, \phi_1 \equiv \theta_3 + \delta + \pi, \tag{70}$$

$$\theta_2 \equiv \phi_3 - \delta, \phi_2 \equiv \phi_3 - \delta + \pi. \tag{71}$$

The solution to the equations exists iff $\delta \in \{\pi/2, 7\pi/6, 11\pi/6\}$ as shown in the top-left plot in figure 8. The eigenvalues shown in the top-left subplot are:

$$\left\{2 + 2\cos\left(\delta + \frac{\pi}{2}\right), 2 + 2\cos\left(\delta - \frac{5\pi}{6}\right), 2 + 2\cos\left(\delta - \frac{\pi}{6}\right)\right\}. \tag{72}$$

Furthermore, we observe that $\mathcal{L}_1^{c,up}$ and $\mathcal{L}_1^{c,down}$ only commute when $\delta = 0$ or π. In figure 9, we illustrate two vector diffusion processes where $\delta = \pi$ and $3\pi/2$. In the top row, the equilibrium vector is the eigenvector associated with a zero eigenvalue for both $\mathcal{L}_1^{c,up}$ and $\mathcal{L}_1^{c,down}$. In the bottom plot, only the vector for $\mathcal{L}_1^{c,down}$ converges to the eigenvector with a zero eigenvalue. For the remaining cases, the final state corresponds to the vector with the smallest positive eigenvalue, given the absence of a zero eigenvalue.

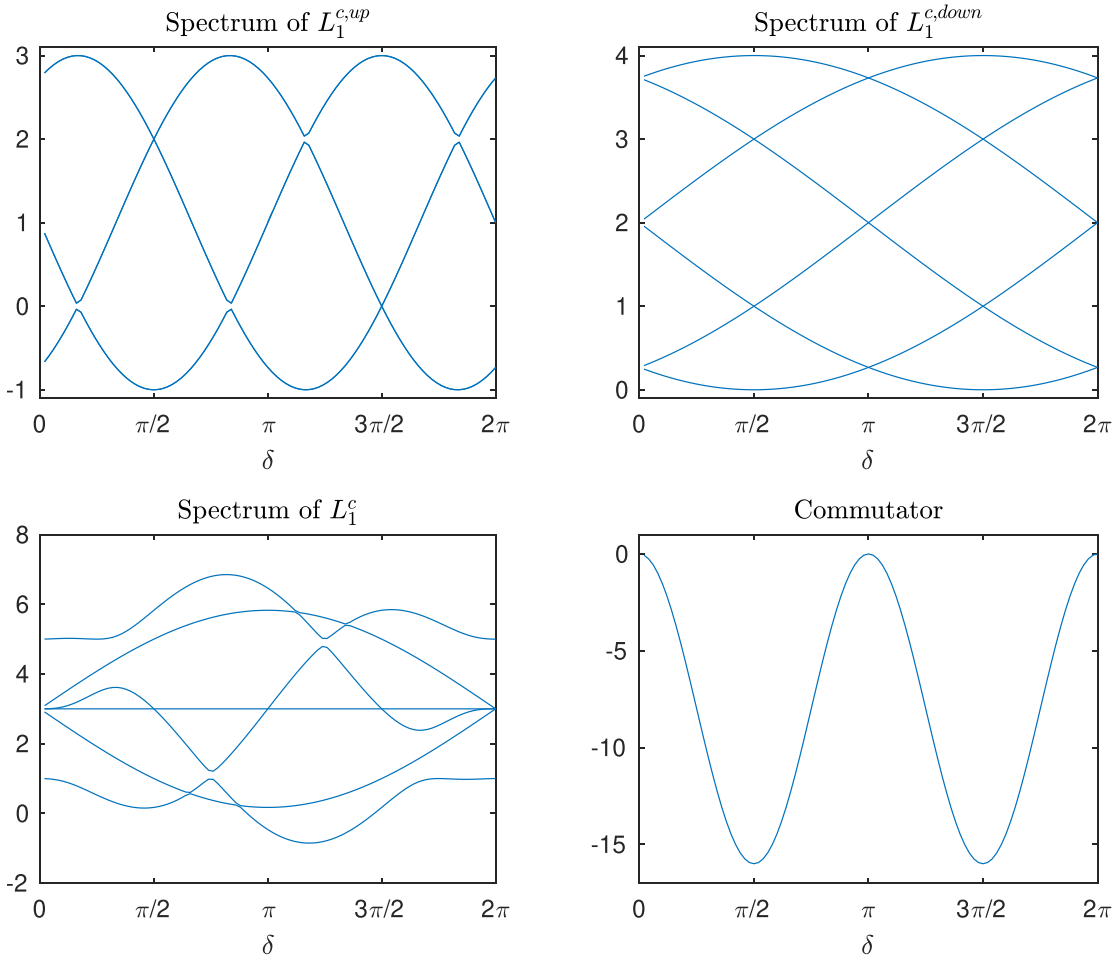

Figure 8. The complete spectra of the 1-Connection Laplacians $\mathcal{L}_1^{c,up}$ (top-left), $\mathcal{L}_1^{c,down}$ (top-right), and $\mathcal{L}_1^c$ (bottom-left), and commutator $[\mathcal{L}_1^{c,up}, \mathcal{L}_1^{c,down}]$(bottom-right) for Case 4 of directed simplicial triangles is plotted as a function of δ.

5.2. Case study on triangulated torus

In the previous examples, we only considered simplicial complexes with a single triangle. Now, we will examine examples where the simplicial complexes contain multiple triangles and edges. Specifically, we will focus on the triangulated torus as our example. The torus is a 2-manifold without boundary. To perform computations, we triangulate the torus into a simplicial complex and we consider two cases that differ only in the direction of the triangles (see figures 10 and 11). For each case, we will investigate the spectrum and the complete spectrum of the 1-up and 1-down Connection Laplacians and we provide a discussion of the effects of the frustration induced by the directions of the simplices.

We first consider the Type 1 Triangulated Torus illustrated in figure 10. In this case, all edge directions align with the triangle directions. Therefore the triangles fall under Case 1 of directed triangles in figure 4.

We then reverse the direction of the upper triangles above the diagonal edges to define the Type 2 Triangulated Torus illustrated in figure 11. As a result, these upper triangles align with Case 2 in figure 4 while the lower triangles correspond to Case 1. Note that for both the Type 1 and the Type 2 Torus we adopt the usual convention for defining the orientations of the edges of their undirected counterpart: instead of taking the orientations induced by the node labels we consider orientations that are consistent with periodic boundary conditions that in these cases are aligned to the direction of the edges depicted in figures 10 and 11.

The effect induced by the frustration of the flow direction is apparent from the comparison among the spectrum of the 1-Connection Laplacians of Type 1 and Type 2 Triangulated Tori (see figures 12 and 13). Indeed for the Type 1 Triangulated Torus it is clearly noticeable that the spectrum displays eigenvalues with much more significant degeneracy than for the Type 2 Triangulated Torus case. Hence in the Type 2 Triangulated Torus, the presence of the frustration induced by the triangle directions lifts the degeneracy of multiple eigenvalues, reflecting a decrease in the symmetries of these directed simplicial complexes.

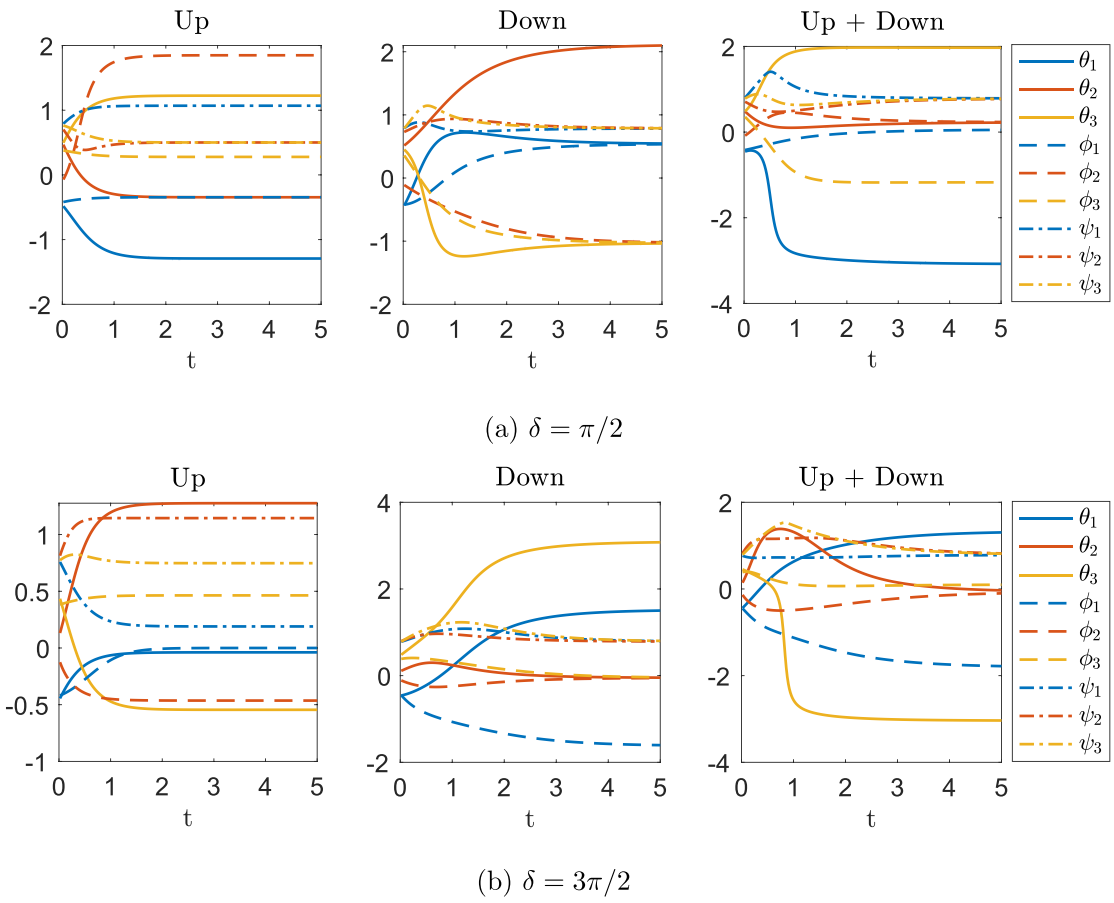

Figure 9. Higher-order diffusion driven by the 1-Connection Laplacians $\mathcal{L}_1^{up}$ (Up), $\mathcal{L}_1^{down}$ (Down) and $\mathcal{L}_1$ (Up+Down) on directed simplicial triangle in Case 4 are plotted for single initial conditions. When $\delta = \pi/3$ (top row), the equilibrium vector coincides with the eigenvector linked to a zero eigenvalue for both $\mathcal{L}_1^{c,up}$ and $\mathcal{L}_1^{c,down}$. Conversely, when $\delta = 2\pi/3$ (bottom row), only the vector associated with $\mathcal{L}_1^{c,down}$ converges towards the eigenvector with a zero eigenvalue. In the remaining scenarios, the final state is determined by the vector possessing the smallest positive eigenvalue.

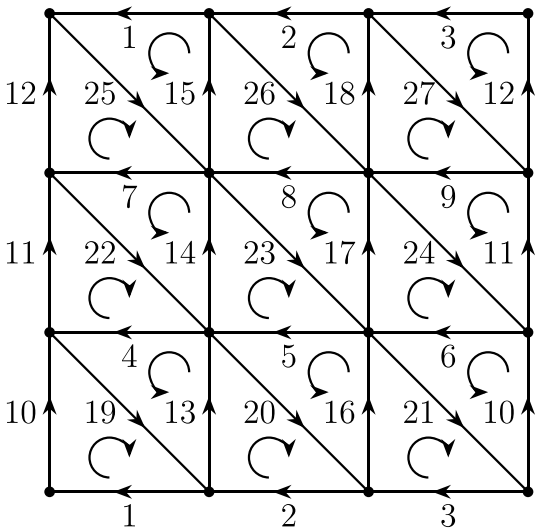

Figure 10. Example of a Type 1 Triangulated Torus of size 3×3 having 25 edges. In this case, there is no frustration as all edge directions align with the triangle directions.

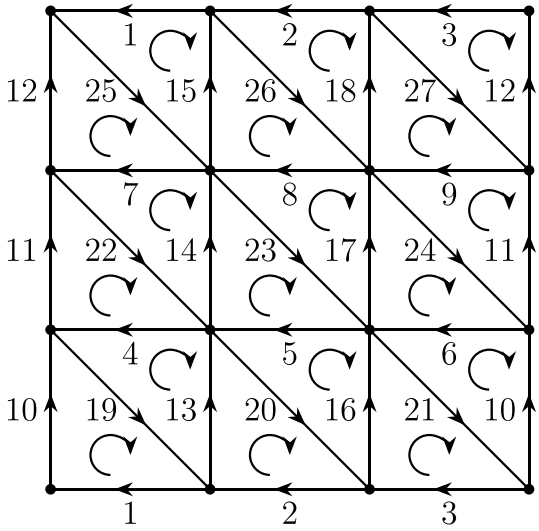

Figure 11. Example of a Type 2 Triangulated Torus of size 3×3 having 25 edges. The flow direction is reversed for all upper triangles above the diagonal edges, as compared to the Type 1 Triangulated Torus.

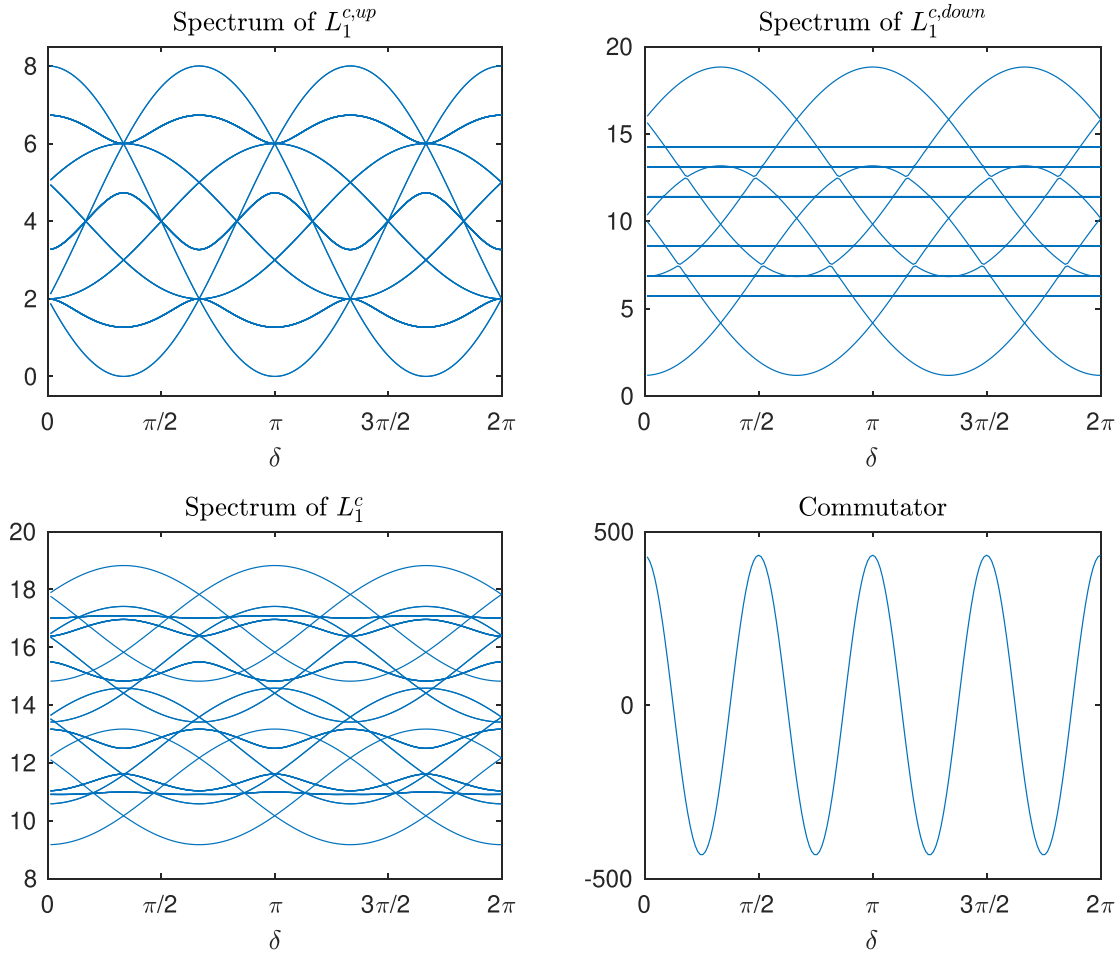

Figure 12. The complete spectra of the 1-Connection Laplacians $\mathcal{L}_1^{c,up}$ (top-left), $\mathcal{L}_1^{c,down}$ (top-right), and $\mathcal{L}_1^{c}$ (bottom-left), and commutator $[\mathcal{L}_1^{c,up}, \mathcal{L}_1^{c,down}]$(bottom-right) for the Type 1 Triangulated Torus of size 3×3 and 25 edges shown in figure 10 are plotted as a function of δ. Note that some eigenvalues are degenerate.

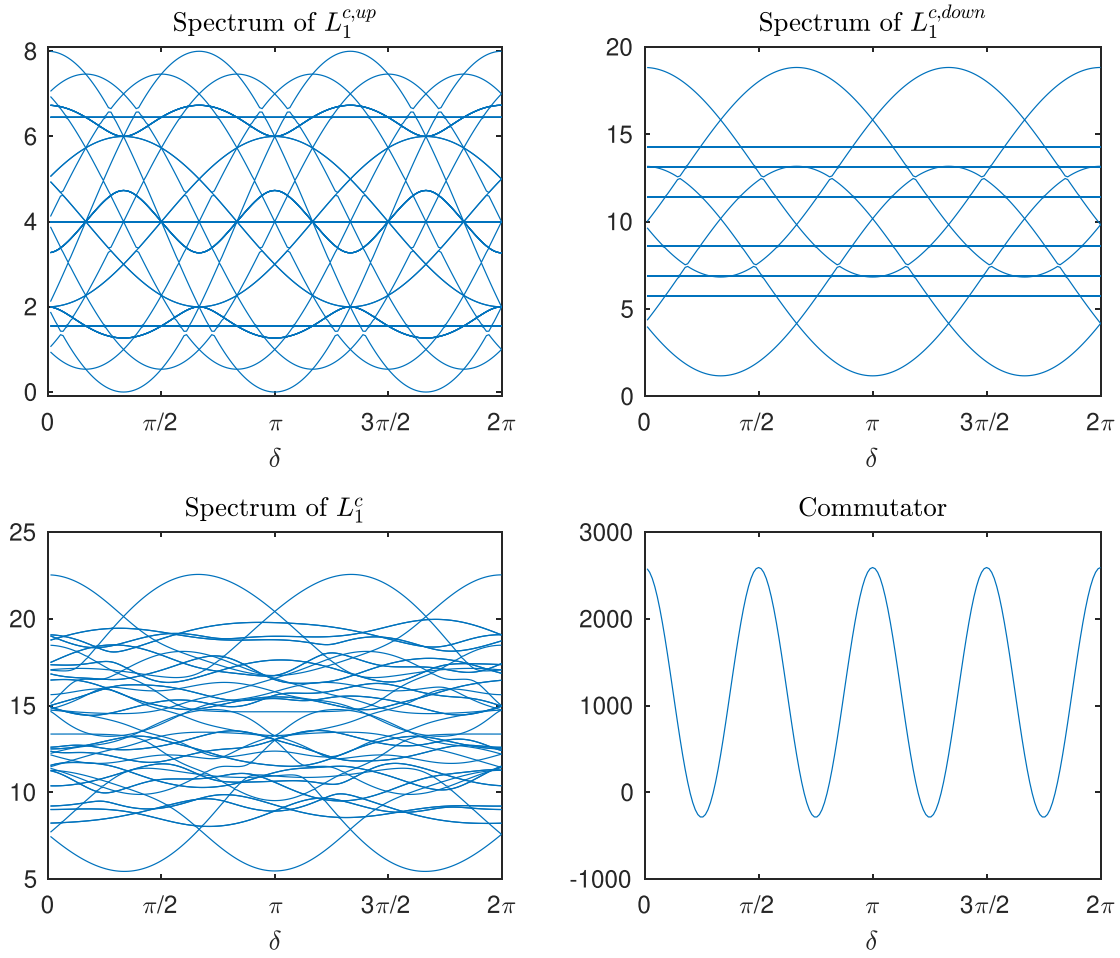

Figure 13. The complete spectra of the 1-Connection Laplacians $\mathcal{L}_1^{c,up}$ (top-left), $\mathcal{L}_1^{c,down}$ (top-right), and $\mathcal{L}_1^c$ (bottom-left), and commutator $[\mathcal{L}_1^{c,up}, \mathcal{L}_1^{c,down}]$(bottom-right) for the Type 2 Triangulated Torus of size 3×3 and 25 edges shown in figure 11 are plotted as a function of δ. Note that some eigenvalues are degenerate but many degeneracies observed in the spectrum of the Type 1 Triangulated Torus are lifted due to the presence of the frustration induced by the directions of the triangles.

6. Conclusion

Directed simplicial complexes constitute an important challenge in network theory as the directionality of interactions is ubiquitous in complex systems. Yet there is not a fully developed mathematical framework for addressing directionality of simplicial complexes. As a matter of fact, so far there is not even consensus on the most suitable definition of directed simplicial complexes. Here we tackle this challenge by leveraging the popular Magnetic Laplacian to address the study of graphs and networks. We show that to formulate corresponding Hermitian operators that can capture all the possible configurations induced by the relative directions of simplices we may consider Higher-order Connection Laplacians making use of the Pauli matrices and of an additional rotation in the complex plane. Specifically, we built the 0-up, 1-up, 1-down, and 2-up Connection Laplacians of tesselations of 2 dimensional orientable manifolds, where the 1-up and 1-down Connection Laplacians can be defined on arbitrary simplicial complexes of any dimensions. The higher-order Connection Laplacians are used to formulate higher-order diffusion dynamics that can capture the frustration induced by incoherent directions of incident simplices. The application of the framework is investigated on simple and instructive examples of 2-dimensional simplicial complexes. In conclusion this work provides a framework for defining directional simplicial complexes and higher-order diffusion dynamics enfolding on them. We build on the increasingly popular idea of adopting complex valued weights to combine dynamical processes on graphs and networks with non-trivial algebraic operations. We hope that this work will be useful for network scientists and applied mathematicians focusing on higher-order networks, complex weights and the interplay between dynamical processes and algebraic operations.

Data availability statement

The data that support the findings of this study are openly available at the following URL/DOI: https://github.com/XueGong-git/Higher-order-Connection-Laplacians [90].

Acknowledgments

This project was carried out during X G's Alan Turing Institute Enrichment Scheme Placement, supported by the Alan Turing Institute. X G acknowledges support of MAC-MIGS CDT under EPSRC Grant EP/S023291/1 and NTU Presidential Postdoctoral Fellowship 023545-00001. D J H was supported by EPSRC Grant EP/P020720/1. K C Z was supported by the Leverhulme Trust Grant 2020-310 and EPSRC Grant EP/V006177/1.

Data, code and materials

Code for the experiments is available at https://github.com/XueGong-git/Higher-order-Connection-Laplacians.

Conflict of interest

The authors declare that they have no conflicts of interest.

ORCID iDs

Xue Gong https://orcid.org/0000-0002-6470-8679
Desmond J Higham https://orcid.org/0000-0002-6635-3461
Konstantinos Zygalakis https://orcid.org/0000-0002-3860-9167
Ginestra Bianconi https://orcid.org/0000-0002-3380-887X

References

[1] Battiston F *et al* 2020 Networks beyond pairwise interactions: structure and dynamics *Phys. Rep.* **874** 1–92
[2] Bick C, Gross E, Harrington H A and Schaub M T 2023 What are higher-order networks? *SIAM Rev.* **65** 686–731
[3] Torres L, Blevins A S, Bassett D and Eliassi-Rad T 2021 The why, how and when of representations for complex systems *SIAM Rev.* **63** 435–85
[4] Salnikov V, Cassese D and Lambiotte R 2018 Simplicial complexes and complex systems *Eur. J. Phys.* **40** 014001
[5] Battiston F *et al* 2021 The physics of higher-order interactions in complex systems *Nat. Phys.* **17** 1093–8
[6] Bianconi G 2021 *Higher Order Networks: An Introduction to Simplicial Complexes* (Cambridge University Press)
[7] Majhi S, Perc M and Ghosh D 2022 Dynamics on higher-order networks: a review *J. R. Soc. Interface* **19** 20220043
[8] Tudisco F and Higham D J 2021 Node and edge nonlinear eigenvector centrality for hypergraphs *Commun. Phys.* **4** 201
[9] Gong X, Higham D J and Zygalakis K 2023 Generative hypergraph models and spectral embedding *Sci. Rep.* **13** 540
[10] Sun H and Bianconi G 2021 Higher-order percolation processes on multiplex hypergraphs *Phys. Rev.* E **104** 034306
[11] Jost J and Mulas R 2019 Hypergraph Laplace operators for chemical reaction networks *Adv. Math.* **351** 870–96
[12] Mulas R, Kuehn C and Jost J 2020 Coupled dynamics on hypergraphs: master stability of steady states and synchronization *Phys. Rev.* E **101** 062313
[13] Carlsson G 2009 Topology and data *Bull. Am. Math. Soc.* **46** 255–308
[14] Vaccarino F, Fugacci U and Scaramuccia S 2022 Persistent homology: a topological tool for higher-interaction systems *Higher-Order Systems* (Springer) pp 97–139
[15] Otter N, Porter M A, Tillmann U, Grindrod P and Harrington H A 2017 A roadmap for the computation of persistent homology *EPJ Data Sci.* **6** 1–38
[16] Ghrist R 2008 Barcodes: the persistent topology of data *Bull. Am. Math. Soc.* **45** 61–75
[17] Meng Z, Anand D V, Lu Y, Wu J and Xia K 2020 Weighted persistent homology for biomolecular data analysis *Sci. Rep.* **10** 2079
[18] Chazal F and Michel B 2021 An introduction to topological data analysis: fundamental and practical aspects for data scientists *Front. Artif. Intell.* **4** 667963
[19] Giusti C, Ghrist R and Bassett D S 2016 Two's company, three (or more) is a simplex: algebraic-topological tools for understanding higher-order structure in neural data *J. Comput. Neurosci.* **41** 1–14
[20] Petri G, Expert P, Turkheimer F, Carhart-Harris R, Nutt D, Hellyer P J and Vaccarino F 2014 Homological scaffolds of brain functional networks *J. R. Soc. Interface* **11** 20140873
[21] Reimann M W, Nolte M, Scolamiero M, Turner K, Perin R, Chindemi G, Dłotko P, Levi R, Hess K and Markram H 2017 Cliques of neurons bound into cavities provide a missing link between structure and function *Front. Comput. Neurosci.* **11** 48
[22] Cang Z, Mu L, Wu K, Opron K, Xia K and Wei G-W 2015 A topological approach for protein classification *Comput. Math. Biophys.* **3** 1
[23] Chan J M, Carlsson G and Rabadan R 2013 Topology of viral evolution *Proc. Natl Acad. Sci.* **110** 18566–71
[24] Nanda V and Sazdanović R 2013 Simplicial models and topological inference in biological systems *Discrete and Topological Models in Molecular Biology* (Springer) pp 109–41
[25] Xia K and Wei G-W 2014 Persistent homology analysis of protein structure, flexibility and folding *Int. J. Numer. Methods Biomed. Eng.* **30** 814–44

[26] De Silva V and Ghrist R 2007 Coverage in sensor networks via persistent homology *Algebr. Geom. Topol.* **7** 339–58
[27] Ghrist R and Muhammad A 2005 Coverage and hole-detection in sensor networks via homology *IPSN 2005. 4th Int. Symp. on Information Processing in Sensor Networks, 2005* (IEEE) pp 254–60
[28] Boksebeld I and Vaxman A 2022 High-order directional fields *ACM Trans. Graph.* **41** 1–17
[29] Zhao R, Desbrun M, Wei G-W and Tong Y 2019 3D Hodge decompositions of edge- and face-based vector fields *ACM Trans. Graph.* **38** 1–13
[30] Millán A P, Torres J J and Bianconi G 2020 Explosive higher-order Kuramoto dynamics on simplicial complexes *Phys. Rev. Lett.* **124** 218301
[31] Arnaudon A, Peach R L, Petri G and Expert P 2022 Connecting Hodge and Sakaguchi-Kuramoto through a mathematical framework for coupled oscillators on simplicial complexes *Commun. Phys.* **5** 211
[32] Calmon L, Restrepo J G, Torres J J and Bianconi G 2022 Dirac synchronization is rhythmic and explosive *Commun. Phys.* **5** 253
[33] Ghorbanchian R, Restrepo J G, Torres J J and Bianconi G 2021 Higher-order simplicial synchronization of coupled topological signals *Commun. Phys.* **4** 120
[34] Nurisso M *et al* 2023 A unified framework for Simplicial Kuramoto models (arXiv:2305.17977)
[35] Torres J J and Bianconi G 2020 Simplicial complexes: higher-order spectral dimension and dynamics *J. Phys. Complex.* **1** 015002
[36] Ziegler C, Skardal P S, Dutta H and Taylor D 2022 Balanced Hodge Laplacians optimize consensus dynamics over simplicial complexes *Chaos* **32** 023128
[37] Schaub M T, Benson A R, Horn P, Lippner G and Jadbabaie A 2020 Random walks on simplicial complexes and the normalized Hodge 1-Laplacian *SIAM Rev.* **62** 353–91
[38] Muhammad A and Egerstedt M 2006 Control using higher order Laplacians in network topologies *Proc. 17th Int. Symp. on Mathematical Theory of Networks and Systems* (Citeseer) pp 1024–38
[39] Barbarossa S and Sardellitti S 2020 Topological signal processing over simplicial complexes *IEEE Trans. Signal Process.* **68** 2992–3007
[40] Schaub M T, Zhu Y, Seby J-B, Roddenberry T M and Segarra S 2021 Signal processing on higher-order networks: Livin'on the edge... and beyond *Signal Process.* **187** 108149
[41] Calmon L, Schaub M T and Bianconi G 2023 Dirac signal processing of higher-order topological signals *New J. Phys.* **25** 093013
[42] Bodnar C *et al* 2021 Weisfeiler and Lehman go topological: message passing simplicial networks *Int. Conf. on Machine Learning* (PMLR) pp 1026–37
[43] Bodnar C, Di Giovanni F, Chamberlain B, Liò P and Bronstein M 2022 Neural sheaf diffusion: a topological perspective on heterophily and oversmoothing in GNNs *Advances in Neural Information Processing Systems* vol 35 pp 18527–41
[44] Eckmann B 1944 Harmonische funktionen und randwertaufgaben in einem komplex *Comment. Math. Helv.* **17** 240–55
[45] Horak D and Jost J 2013 Spectra of combinatorial Laplace operators on simplicial complexes *Adv. Math.* **244** 303–36
[46] Lim L-H 2020 Hodge Laplacians on graphs *SIAM Rev.* **62** 685–715
[47] Courtney O T and Bianconi G 2018 Dense power-law networks and simplicial complexes *Phys. Rev.* E **97** 052303
[48] Méndez D and Sńchez-García R J 2023 A directed persistent homology theory for dissimilarity functions *J. Appl. Comput. Topol.* **7** 771–813
[49] Grigor'yan A A, Lin Y, Muranov Y V and Yau S-T 2020 Path complexes and their homologies *J. Math. Sci.* **248** 564–99
[50] Suwayyid F and Wei G W 2023 Persistent Dirac of path and hypergraph (arXiv:2311.14893)
[51] Shubin M 1998 Discrete magnetic Laplacian *Commun. Math. Phys.* **164** 259–75
[52] Kogut J B 1979 An introduction to lattice gauge theory and spin systems *Rev. Mod. Phys.* **51** 659
[53] Kogut J and Susskind L 1975 Hamiltonian formulation of Wilson's lattice gauge theories *Phys. Rev.* D **11** 395
[54] Lieb E H and Loss M F 1993 Laplacians and Kasteleyn's theorem *Statistical Mechanics: Selecta of Elliott H. Lieb* (Springer) pp 457–83
[55] Fanuel M, Alaiz C M, Fernandez A and Suykens J A K 2018 Magnetic Eigenmaps for the visualization of directed networks *Appl. Comput. Harmon. Anal.* **44** 189–99
[56] Lange C, Liu S, Peyerimhoff N and Post O 2015 Frustration index and Cheeger inequalities for discrete and continuous magnetic Laplacians *Calc. Var. Partial Differ. Equ.* **54** 4165–96
[57] Fanuel M, Alaíz C M and Suykens J A K 2017 Magnetic Eigenmaps for community detection in directed networks *Phys. Rev.* E **95** 022302
[58] Gong X, Higham D J and Zygalakis K 2021 Directed network Laplacians and random graph models *R. Soc. Open Sci.* **8** 211144
[59] Tian Y and Lambiotte R 2023 Structural balance and random walks on complex networks with complex weights (arXiv:2307.01813)
[60] Zhang X, He Y, Brugnone N, Perlmutter M and Hirn M 2021 Magnet: a neural network for directed graphs *Advances in Neural Information Processing Systems* vol 34 pp 27003–15
[61] Böttcher L and Porter M A 2024 Complex networks with complex weights *Phys. Rev.* E **109** 024314
[62] Böttcher L and Porter M A 2024 Dynamical processes on metric networks (arXiv:2401.00735)
[63] Singer A and Wu H 2012 Vector diffusion maps and the connection Laplacian *Commun. Pure Appl. Math.* **65** 1067–144
[64] Bandeira A S, Singer A and Spielman D A 2013 A Cheeger inequality for the graph connection Laplacian *SIAM J. Matrix Anal. Appl.* **34** 1611–30
[65] Chung F and Kempton M 2013 A local clustering algorithm for connection graphs *Algorithms and Models for the Web Graph: 10th Int. Workshop, WAW 2013 (Cambridge, MA, USA, 14–15 December 2013 (Proc.)* (Springer) pp 26–43
[66] Bianconi G 2021 The topological Dirac equation of networks and simplicial complexes *J. Phys. Complex.* **2** 035022
[67] Muolo R, Carletti T and Bianconi G 2024 The three way Dirac operator and dynamical Turing and Dirac induced patterns on nodes and links *Chaos Solitons Fractals* **178** 114312
[68] Lohe M 2010 Quantum synchronization over quantum networks *J. Phys. A: Math. Theor.* **43** 465301
[69] Lohe M 2021 Higher-order synchronization on the sphere *J. Phys. Complex.* **3** 015003
[70] Hansen J and Ghrist R 2021 Opinion dynamics on discourse sheaves *SIAM J. Appl. Math.* **81** 2033–60
[71] Barbero F, Bodnar C, de Ocáriz Borde H S, Bronstein M, Veličković P and Lio P 2022 Sheaf neural networks with connection Laplacians *Topological, Algebraic and Geometric Learning Workshops 2022* (PMLR) pp 28–36
[72] Böttcher L and Porter M A 2021 Classical and quantum random-walk centrality measures in multilayer networks *SIAM J. Appl. Math.* **81** 2704–24
[73] Luxburg U 2007 A tutorial on spectral clustering *Stat. Comput.* **17** 395–416
[74] Banerjee A and Jost J 2008 On the spectrum of the normalized graph Laplacian *Linear Algebr. Appl.* **428** 3015–22
[75] Von Luxburg U, Belkin M and Bousquet O 2008 Consistency of spectral clustering *Ann. Stat.* **36** 555–86
[76] Chung F 1997 *Spectral Graph Theory* (*Regional Conference Series in Mathematics* vol 92) (American Mathematical Society)

[77] White S and Smyth P 2005 A spectral clustering approach to finding communities in graphs *Proc. 2005 SIAM Int. Conf. on Data Mining* (SIAM) pp 274–85
[78] Higham D J, Kalna G and Kibble M J 2007 Spectral clustering and its use in bioinformatics *J. Comput. Appl. Math.* **204** 25–37
[79] Lambiotte R and Schaub M T 2022 *Modularity and Dynamics on Complex Networks. Elements in the Structure and Dynamics of Complex Networks* (Cambridge University Press)
[80] Krishnagopal S and Bianconi G 2021 Spectral detection of simplicial communities via Hodge Laplacians *Phys. Rev.* E **104** 064303
[81] Roddenberry T M, Frantzen F, Schaub M T and Segarra S 2022 Hodgelets: localized spectral representations of flows on simplicial complexes *ICASSP 2022-2022 IEEE Int. Conf. on Acoustics, Speech and Signal Processing (ICASSP)* (IEEE) pp 5922–6
[82] Cucuringu M 2016 Sync-rank: robust ranking, constrained ranking and rank aggregation via eigenvector and SDP synchronization *IEEE Trans. Netw. Sci. Eng.* **3** 58–79
[83] Ng A, Jordan M and Weiss Y 2001 On spectral clustering: analysis and an algorithm *Advances in Neural Information Processing Systems* vol 14
[84] Wang C D and Lai J H 2016 Nonlinear clustering: methods and applications *Unsupervised Learning Algorithms* (Springer International Publishing) pp 253–302
[85] He Y H and Yau S T 2020 Graph Laplacians, Riemannian manifolds and their machine-learning (arXiv:2006.16619)
[86] Chung F and Zhao W 2012 Ranking and sparsifying a connection graph *Algorithms and Models for the Web Graph* (*Lecture Notes in Computer Science* vol 7323) (Springer) pp 66–77
[87] Hoff P D, Raftery A E and Handcock M S 2002 Latent space approaches to social network analysis *J. Am. Stat. Assoc.* **97** 1090–8
[88] Forman R 2003 Bochner's method for cell complexes and combinatorial Ricci curvature *Discrete Comput. Geom.* **29** 323–74
[89] Taylor D, Klimm F, Harrington H A, Kramár M, Mischaikow K, Porter M A and Mucha P J 2015 Topological data analysis of contagion maps for examining spreading processes on networks *Nat. Commun.* **6** 7723
[90] Gong X 2023 Higher-order-Connection-Laplacians (available at: https://github.com/XueGong-git/Higher-order-Connection-Laplacians)